Detecting Foundation Pile Length of High-Mast Light Towers

Bojan Guzina, Principal Investigator
Department of Civil, Environmental, and Geo- Engineering

AUGUST 2022

Technical Report Documentation Page

1. Report No. MN 2022-28	2.	3. Recipients Accession No.	
Detecting Foundation Pile Length of High-Mast Light Towers		5. Report Date August 2022	
		6.	
7. Author(s) Daniel Kennedy, Bojan Guzina, Joseph Labuz		8. Performing Organization Report No.	
9. Performing Organization Name and Address Department of Civil, Environmental, and Geo- Engineering University of Minnesota 500 Pillsbury Drive S.E. Minneapolis, MN 55455-0116		10. Project/Task/Work Unit No. #2019003	
		11. Contract (C) or Grant (G) No. (c) 1006625 (wo) 62	
12. Sponsoring Organization Name and Address Minnesota Department of Transportation Office of Research & Innovation 395 John Ireland Boulevard, MS 330 St. Paul, Minnesota 55155-1899		13. Type of Report and Period Covered Final Report	
		14. Sponsoring Agency Code	

16. Abstract (Limit: 250 words)

The goal of the project is to establish a non-destructive field testing technique, including a data analysis algorithm, for determining in-place pile lengths by way of seismic waves. The length of each pile supporting a high-mast light tower (HMLT) will be identified through a systematic sensing approach that includes (i) collection and classification of the pertinent foundation designs and soil conditions; (ii) use of ground vibration waveforms captured by a seismic cone penetrometer; (iii) three-dimensional visco-elastodynamic finite element analysis (FEA) used as a tool to relate the sensory data to in situ pile length; (iv) use of machine learning (ML) algorithms, trained with the outputs of FEA simulations, to solve the germane inverse problem; (v) HMLT field testing; and (vi) analysis-driven data interpretation. Several hundred HMLTs throughout Minnesota have foundation systems, typically concrete-filled steel pipe piles or steel H-piles, with no construction documentation (*e.g.,* pile lengths). Reviews of designs within current standards suggest that some of these foundations may have insufficient uplift capacity in the event of peak wind loads. Without knowledge of the in situ pile length, an expensive retrofit or replacement program would need to be conducted. Thus, developing a screening tool to determine in situ pile length — as compared to a bulk retrofit of all towers with unknown foundations — would provide significant cost savings.

17. Document Analysis/Descriptors Nondestructive tests, Piles (Supports), Depth, Machine learning, High mast lighting		18. Availability Statement No restrictions. Document available from: National Technical Information Services, Alexandria, Virginia 22312	
19. Security Class (this report) Classified	20. Security Class (this page) Unclassified	21. No. of Pages 46	22. Price

Detecting Foundation Pile Lengths of High-Mast Light Towers

FINAL REPORT

Prepared by:

Daniel V. Kennedy
Bojan B. Guzina
Joseph F. Labuz
Department of Civil, Environmental, and Geo- Engineering
University of Minnesota

August 2022

ACKNOWLEDGMENTS

TABLE OF CONTENTS

LIST OF FIGURES

LIST OF TABLES

EXECUTIVE SUMMARY

This report establishes non-destructive field-testing techniques, including a data analysis algorithm, for determining in situ foundation pile embedment depths by way of seismic waves. The embedment depth of each pile supporting a high mast light tower (HMLT) is identified through a systematic sensing approach that includes (i) collection and classification of pertinent foundation designs and soil conditions; (ii) 3D simulations of dynamic soil-foundation interaction; (iii) parametric studies of the 3D pile sensing problem; (iv) field testing, and (v) synthetic data-driven interpretation of the field measurements by way of machine learning (ML) algorithms.

Chapter 1 highlights the tower foundation geometry and research motivation. It is estimated that a potential benefit to Minnesota taxpayers of more than $8 million in unnecessary foundation replacement costs could be realized with the development of non-destructive evaluation (NDE) techniques for determining the in situ pile lengths of the deep foundation.

Chapter 2 introduces two testing methodologies: (i) steady-state vibration source and (ii) hammer impact. The key in the development of the method is the recognition that each foundation pile serves, thanks to high impedance contrast between the pile and soil, both as a *waveguide*, facilitating the transmission of mechanical energy all the way to the bottom of the pile, and as a *mechanical antenna*, where the wave energy propagating down the pile is partially radiated into the surrounding soil. For enhanced robustness of the pile depth estimates, the envisioned field procedure entails the application of both transient (i.e. hammer impact) and steady-state (i.e. shaker) excitation of the pile cap, while monitoring the induced ground motion via seismic cone penetrometer (SCP) along a vertical line close to the pile being interrogated. Normalization and signal filtering of the field data are introduced to produce quantifiable outputs from the two testing methods and eliminate unwanted electrical, environment, and sensor background noises.

Chapter 3 presents the finite element analysis (FEA) computational platform used for numerical simulations of the NDE soil-structure interaction. For the simulations, two methods of analysis are carried out: (i) time-harmonic steady-state solution to match the vibratory shaker sensing method and (ii) transient time-dependent solution for the hammer impact sensing method. To capture the inherent parametric variability of the HMLT foundation setup, hundreds of finite element simulations are performed generating thousands of synthetic neural network training data points that span different analysis methods (steady-state vs. transient), excitation frequencies, SCP observation locations, pile lengths, soil conditions, and foundation geometries. This section also includes an analytical validation of the time-invariant steady-state FEA model, giving confidence in the numerical solutions.

Chapter 4 focuses on the implementation of machine learning (ML) algorithms that provide the back-analyses of both steady-state and transient synthetic data. The featured ML algorithms are implemented as deep neural networks within the *Keras* and *TensorFlow* computational environment to enable a robust yet computationally efficient interpretation of the vibratory and hammer impact data. Results from the neural networks show low error values and high goodness-to-fit, in terms of estimated pile depth, when applied to (synthetic) validation, i.e. test data.

Chapter 5 provides results from field testing of HMLT foundations. Multiple HMLT foundations in the Twin Cities metro area were successfully tested from September 2020 to June 2022. During the testing, both steady state and hammer impact testing methods were implemented to determine the pile embedment depth of the tower foundations. To prepare the site for field testing, a preliminary investigation procedure was developed and implemented, providing the orientation and geometry of the in-ground pile cap, thus giving guidance on optimal locations for the testing hardware and SCP truck.

- The results obtained for HMLT E3A-11 in Mendota Heights, Minnesota, show a clear and significant change in the ground motion for both testing methods at depths between 10 m and 11 m.
- Comparing the pile length estimates obtained by field testing to those provided by MnDOT's High Mast Light Tower database MDH excel file shows that the estimates obtained during testing at HMLT W1L-5 in Burnsville, Minnesota, closely matched the expected pile depth for the hammer impact method and were less conclusive for the vibratory source method.
- Results from testing at HMLT R19J-7 in Shakopee, Minnesota, show that the hammer impact analysis for Pile 1 yields both: (i) repeatable results (tested in November 2021 and retested in May 2022), and (ii) in situ estimates that match closely the expected pile length. For Pile 1 of HMLT R19J-7, however, the back-analysis of the vibratory field data is less conclusive. For Pile 2 of HMLT R19J-7, on the other hand, both the hammer impact and vibratory source analyses give pile depth estimates that are mutually consistent, yet roughly 2 to 2.5 m shorter than the expected pile embedment depth.
- Given the apparent drawbacks of the vibratory testing approach, the field testing of HMLT S4F-17 in Eden Prairie, Minnesota, focused exclusively on the hammer impact analysis. It was demonstrated that traditional once penetration testing (CPT) and the hammer impact evaluation of all three piles for HMLT S4F-17 could be conducted in a single day. Outputs from the hammer impact analysis of HMLT S4F-17 showed a good match between the predicted and expected pile depth for the SE pile, while the NE and W piles have predicted depths that were somewhat deeper than expected.
- A second tower, HMLT S4F-15, in Eden Prairie, Minnesota, was also evaluated using only the hammer impact method. The results from the field testing and corresponding output from the ML neural network showed a close match between predicted and expected pile end depth.

Overall, the results show that the hammer impact method of analysis seems to provide closer and more consistent outputs for the in situ depth of HMLT foundations than the vibratory method. In addition, the results show that by only implementing the hammer impact method, an entire HMLT (3 piles) can be nondestructively evaluated, including performing CPT soil analysis, in a single day of testing.

CHAPTER 1: INTRODUCTION

Several hundred high mast light towers (HMLTs) throughout Minnesota have foundation systems, typically concrete-filled steel pipe piles or steel H-piles, with no recorded pile lengths. Reviews of designs within current standards suggest that some of these foundations could have insufficient uplift capacity in the event of peak wind loads. Without knowledge of the in situ pile length, an expensive retrofit or replacement program would need to be conducted. Thus, developing a screening tool to determine in situ pile length — as compared to a bulk retrofit of all towers with unknown foundations — would provide significant cost savings. The goal of the project is to establish a non-destructive evaluation (NDE) technique, including the testing setup and data analysis algorithms, for determining in situ pile lengths by way of seismic waves.

The work contained in this report is specifically focused on: (i) collection and classification of the pertinent foundation designs and soil conditions; (ii) use of ground vibration waveforms captured by a seismic cone penetrometer; (iii) three-dimensional visco-elastodynamic finite element analysis (FEA) used as a tool to relate the sensory data to pile length; (iv) use of machine learning (ML) algorithms, trained with the outputs of FEA simulations, to solve the germane inverse problem; (v) HMLT field testing; and (vi) analysis-driven data interpretation. In principle, the scarcity of existing HMLT configurations with known pile depth creates an absence of field data needed to adequately train an ML algorithm. However, it will be demonstrated that the use of FEA simulations as proxy training data for the ML algorithms leads to a robust data interpretation scheme.

An HMLT is a tall, thin, tapered steel pole with downward facing lights attached at the top (Fig. 1.1). Typically, HMLTs are designed to reach heights of between 30.5 m (100 ft) and 42.7 m (140 ft) and work in unison with other towers or light sources to achieve the necessary level of illumination. High activity areas including freeways, intersections, and airports require additional safety provisions concerning visibility. Typically, these locations also need to use the available land area in the most efficient manner. To achieve this, HMLTs can illuminate large surface areas while maintaining a small footprint.

With reference to Fig. 1.2, pile supported HMLT foundation systems typically consist of three inclined concrete-filled steel pipe piles or steel H-piles that connect to the light tower via a triangular concrete pile cap. Because the tower behaves structurally as a tall cantilever, its foundation system needs to provide sufficient resistance to overturning moments due to peak wind load, in addition to necessary bearing capacity. Overturning moments and forces produced by wind load are resisted by both the bearing and uplift capacities of the embedded piles, which increase with the piles' embedment length. Table 1.1 shows the key geometric differences between the three types of tower bases.

Figure 1.1 High mast light towers.
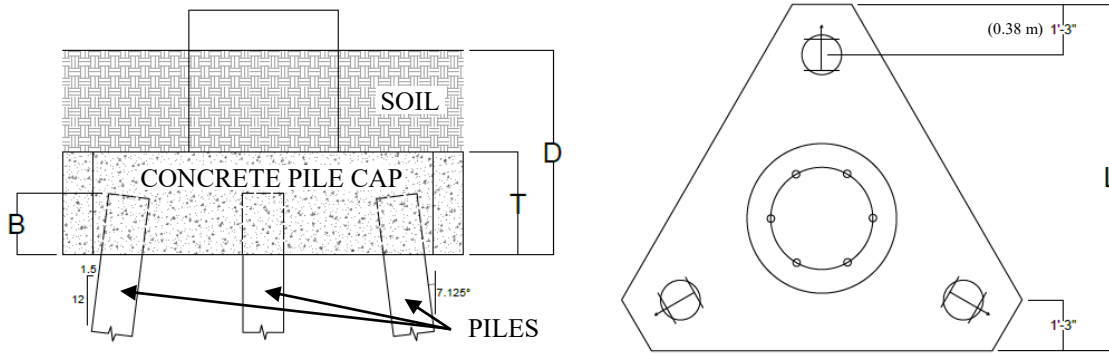
Figure 1.2 Typical HMLT foundation geometry (cross section and plan view).

Table 1.1 Foundation geometry values for typical designs.

Type	L	B	T	D	Tower Height
T-100	8'-6" (2.6 m)	1'-6" (0.46 m)	2'-6" (0.76 m)	5'-0" (1.52 m) ±	100' (30.48 m)
T-120	11'-6" (3.5 m)	2'-0" (0.61 m)	3'-6" (1.07 m)	6'-0" (1.83 m) ±	120' (36.58 m)
T-140	11'-6" (3.5 m)	2'-0" (0.61 m)	3'-6" (1.07 m)	6'-0" (1.83 m) ±	140' (42.67 m)

1.1 ESTIMATE OF BENEFITS TO MINNESOTA TAXPAYERS

According to current estimates, there are 235 HMLTs in Minnesota (over 50% of the 442 towers in the state) with no construction records indicating the pile length. Many of these HMLTs have no on-site soil information either. Numerical simulations suggest that during peak wind loading, the HMLT foundation may not have sufficient uplift capacity. The cost estimate to retrofit or replace each individual HMLT foundation, with unknown pile length, is approximately $40,000, not including costs associated with salvaging or reinstalling the tower. If the unknown pile lengths could be determined and were found to be adequate, then the tower foundations would not require a retrofit or replacement.

During field testing of the tower foundations, it was demonstrated that it is reasonable to expect that one foundation pile could be tested per day, indicating that it would take up to three days of testing for one complete tower foundation with three inclined piles. However, with more crew training and increased testing efficiency, it is expected that up to two foundation piles may be tested per day. The daily cost for cone penetration testing (CPT) and crew is approximately $1,500 and the post-processing of three foundation pile field tests is estimated to take on the order of two days, assuming that it is processed by a single employee. This suggests that the cost to test an individual tower foundation with three piles is $5,000 ($4,500 for the CPT and an estimated $500 for two days of post-processing personnel costs).

Table 1.2 indicates that a possible benefit to Minnesota taxpayers of more than $8 million in foundation replacement costs (including tower testing and post-processing costs) could be realized with the development of non-destructive evaluation (NDE) techniques for determining the in situ pile lengths of the deep foundation if none of the tested HMLTs were to require additional work. Assuming, on the other hand, that 50% of the HMLTs tested have insufficient pile length, i.e. uplift capacity, estimated savings to the Minnesota taxpayers would likely still be more than $3.5 million.

Table 1.2 Benefits to Minnesota taxpayers.

HMLT Costs		Benefits to Minnesota Taxpayers		
# of Foundations: 235		Based on % of tested towers requiring additional work:		
Testing Costs	Cost Per Replacement	0%	25%	50%
$5,000	$40,000	$8,225,000	$5,875,000	$3,525,000

CHAPTER 2: PILE SENSING METHODOLOGY

The research project deals with the establishment and implementation of NDE field testing techniques, including data analysis algorithms, for determining in situ pile lengths by way of seismic waves. The length of each pile supporting an HMLT is identified through a systematic sensing approach that includes (i) collection and classification of pertinent foundation designs and soil conditions; (ii) three-dimensional (3D) simulations of dynamic soil-foundation interaction; (iii) parametric studies of the 3D pile sensing problem; (iv) field testing, and (v) analysis driven data interpretation using machine learning (ML) algorithms.

Figure 2.1 illustrates the proposed testing setup for estimating the in situ pile depth: a vertical mechanical excitation is applied to the pile cap above (or near) the pile stem, while the geophones mounted near the tip of an advancing seismic cone penetrometer (SCP), pushed into the ground by a cone penetration testing (CPT) rig, are used to monitor the induced (near-field) ground movement. At each observation depth, the pile cap is excited in sequence by (i) steady-state vibration generated by a pneumatic shaker, and (ii) hammer impact. A physical connection between the vibration source and the pile cap is provided by a steel rod driven into the topsoil. The use of two distinct vibration sources is motivated by the need for two independent methodologies, i.e. inversion schemes, for assessing the in situ pile length. Measurements of the ground motion at several observation depths along a vertical line near the pile are recorded. The seismic data are then processed and "compared", via an ML algorithm, to the outputs of numerical simulations and previously tested foundations to determine the pile length. In the proposed NDE scheme, both steady-state vibration and hammer impact responses are deployed for their complementary performance in complex/noisy environments. Accordingly, they each necessitate the development of a custom ML data interpretation scheme, and each provides an independent assessment of the in situ pile length.
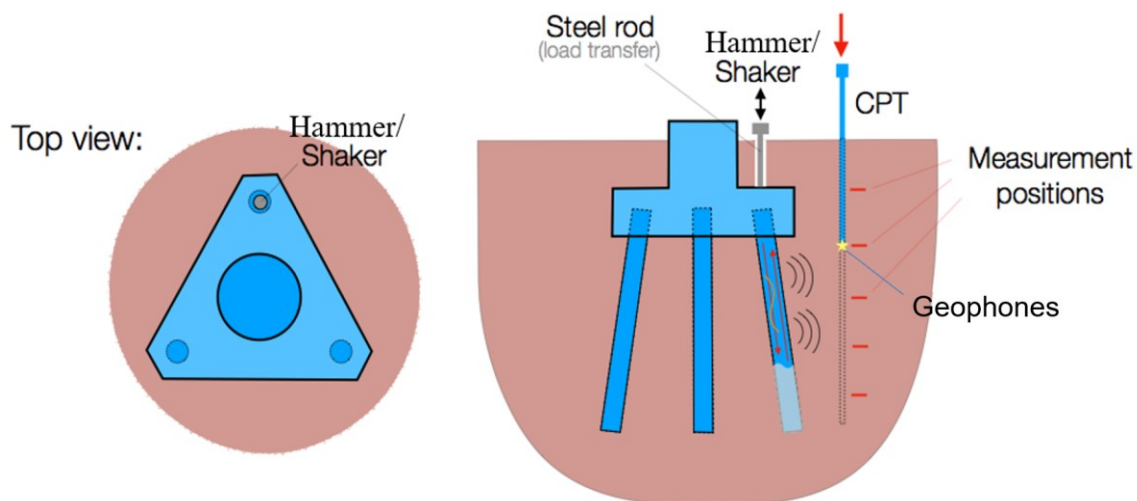
Figure 2.1 Schematics of the pile sensing approach.

The essence of both the steady-state vibration and hammer impact methods are the fact that each foundation pile serves, thanks to high impedance contrast between the pile and soil, as a *waveguide*,

facilitating the transmission of mechanical energy all the way to the bottom of the pile, and as a *mechanical antenna*, where the wave energy propagating down the pile is partially radiated into the surrounding soil. This latter part of the elastic wave energy is then picked up by a geophone mounted near the tip of an SCP device and provides the data from which the pile length is evaluated.

2.1 STEADY-STATE VIBRATORY SHAKER METHOD

The vibratory shaker method of pile depth analysis uses steady state vibrations. The pile movement in the ground is initiated by a pneumatic piston vibratory shaker secured to a metal rod via a bolted mounting plate, as shown in Figure 2.2. The metal rod is pushed into the soil and contacts the top of the pile cap, directly over its contact with the pile of interest.

Figure 2.2 Pneumatic vibratory shaker device configuration.

While the vibratory shaker is in operation, a digital signal analyzer (DSA) is activated to record the ground motion of the geophones at the testing depth. The record of ground motion is analyzed using the Fourier transform (FT) to provide the magnitude of the signal's frequency components. Figure 2.3 shows the vibration signal in time domain (top image) and frequency domain (bottom image) for a typical steady state vibration test. Figure 2.4 displays an enlarged view of the frequency domain near the frequency of excitation, including sensor labels and the components of ground motion captured by each sensor.
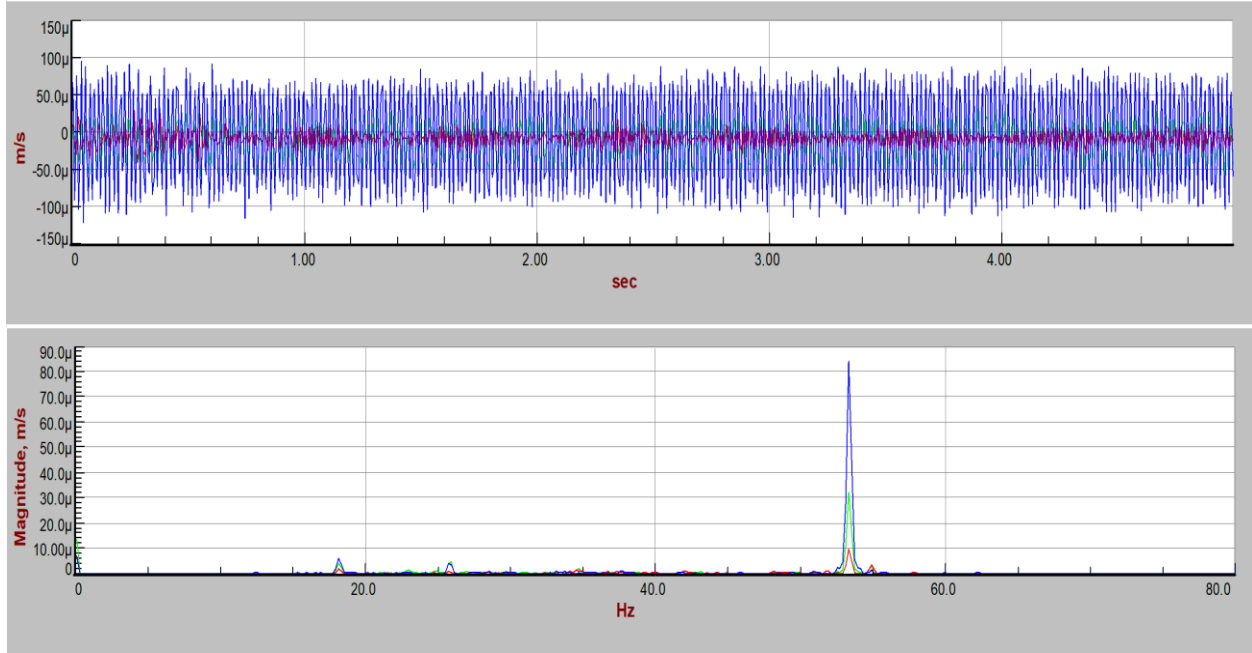
Figure 2.3 Time (top) and frequency (bottom) domain representation of vibration signal.
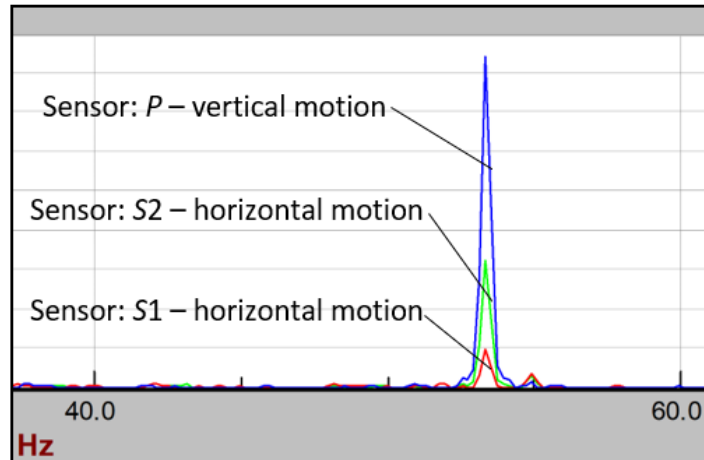
Figure 2.4 Three-dimensional components of captured ground motion.

The overall magnitude of the ground motion induced by the vibratory shakers

$$\|v\| = (P^2 + S1^2 + S2^2)^{1/2} \tag{1}$$

is computed at each test depth. Up to five recordings were taken at each depth, with the average value being used to reduce background noise.

Once obtained, the results of the overall ground motion are normalized so that the L2-norm of the ground motion profile is unity. Specifically, letting $z_1, z_2, \ldots, z_n$ be the sensing depths and arranging the data in a vector of magnitudes as $V = (\|v(z_1)\|, \|v(z_2)\|, \ldots, \|v(z_n)\|)$, we normalize the sensory data as

$$V_n = \frac{V}{\sqrt{V^T V}}, \quad \|V_n\|_2 = 1. \tag{2}$$

6

To understand the influence of the pile's end depth on the ground motion, the normalized ground motion magnitude is plotted vs. cone test depth, shown in Figure 2.5. Numerical simulations indicate that a drop in ground motion response is expected near the pile end depth.
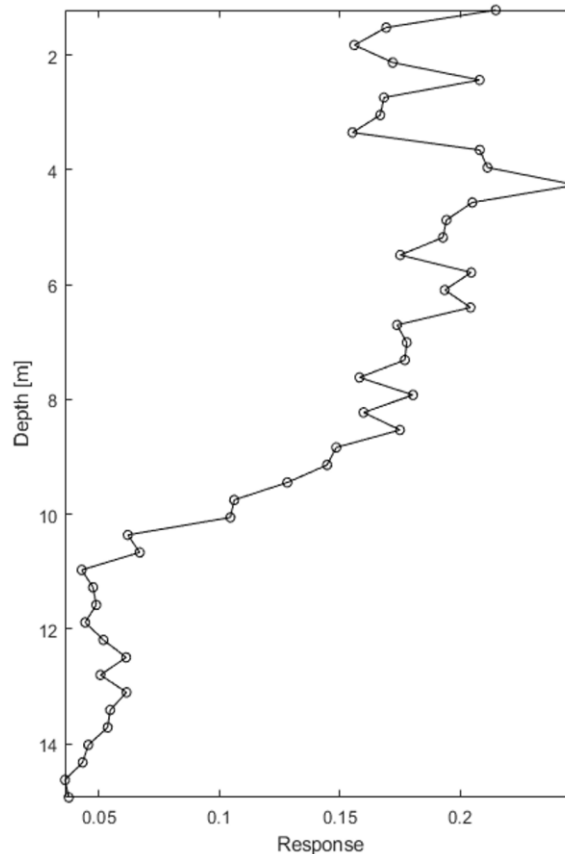
Figure 2.5 Normalized ground motion vector vs. testing depth.

2.2 TRANSIENT HAMMER IMPACT METHOD

The hammer impact method of pile analysis uses a single hammer impact on the top of the mounting plate, transferring the compression wave into the pile through the pile cap. Figure 2.6 shows the hammer impact configuration, including an 8.9x8.9x8.9 cm (3.5x3.5x3.5 in.) wooden block used between the hammer and mounting plate to transfer the impact and protect the testing hardware. The DSA software is triggered the moment the mounting plate is impacted via an accelerometer attached to the hammer. Once the DSA is triggered by the hammer impact, the SCP geophone sensor signal is recorded for a sufficient time to capture the first wave arrival and ensuing motion of the pile and surrounding soil.

Figure 2.6 Hammer impact method configuration.

Figure 2.7 details the process by which the impact ground signals are filtered and displayed: (a) the original ground signal; (b) band-stop filters applied to remove background electrical noise[1]; (c) multiple filtered signal recordings are stacked to find the averaged signal; (d) the resulting averaged time signal; (e) the averaged signals, at each depth, are scaled and cascaded; and, (f) the final cascade plot after a bandpass filter removes the natural oscillations of the geophone sensor[2].

1. Circled with red in Figure 2.7 (a).
2. Natural resonant frequency of the geophone is 28 Hz.
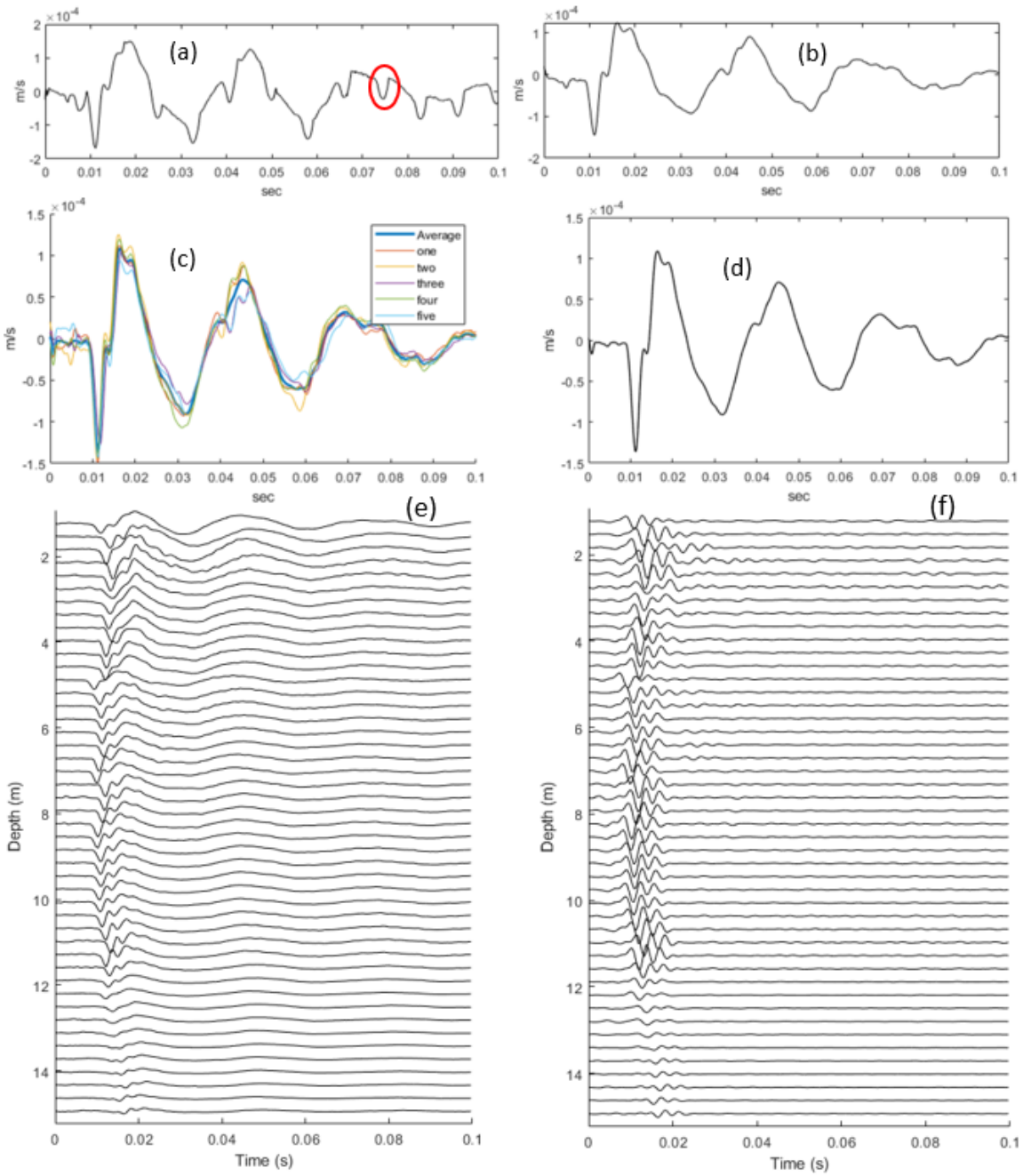
Figure 2.7 Hammer impact data processing steps.

CHAPTER 3: FINITE ELEMENT MODEL AND SIMULATIONS

3.1 VISCO-ELASTODYNAMIC MODELING

An open-source FEA platform, *Code_Aster* [1, 2, 3], was chosen to simulate and analyze the ground motion involved in detecting the in situ length of the foundation piles. *Code_Aster* was mainly developed by the research and development group at Électricité de France, a large electric utility operated by the French government. The software provides a platform for numerical simulations over a wide range of applications including thermal, mechanical, and acoustic problems, both in terms of transient and steady-state simulations.

On discretizing the solid region of interest via finite elements, *Code_Aster* converts the governing field equations (balance of linear momentum) subject to appropriate boundary conditions into an algebraic system of equations:

$$\boldsymbol{M}\ddot{\boldsymbol{u}}(t) + \boldsymbol{C}\dot{\boldsymbol{u}}(t) + \boldsymbol{K}\boldsymbol{u}(t) = \boldsymbol{f}(t) \tag{3}$$

that are solved in terms of a time-dependent displacement vector, $\boldsymbol{u}(t)$, that is directly relevant to the hammer impact analysis. Here $\boldsymbol{M}$, $\boldsymbol{C}$ and $\boldsymbol{K}$ are the system's mass, damping, and stiffness matrices, respectively, overdot denotes time derivative, $\boldsymbol{u}$ collects the nodal displacements, and $\boldsymbol{f}$ is the vector synthesizing applied loads. In this study, $\boldsymbol{C}$ is constructed via the Rayleigh damping model, $\boldsymbol{C} = \alpha\boldsymbol{K} + \mu\boldsymbol{M}$, where α and μ quantify respectively the stiffness- and mass-proportional contributions to the damping matrix. *Code_Aster* uses the Newmark method [4, 5] with $\gamma = 1/2$ and $\beta = 1/4$ to solve for the time-dependent displacement vector, $\boldsymbol{u}(t)$.

For time-harmonic excitation with implicit temporal dependence, $e^{i\omega t}$, that is relevant to the shaker analysis, (3) can be rewritten as

$$(-\omega^2\boldsymbol{M} + i\omega\boldsymbol{C} + \boldsymbol{K})\boldsymbol{U} = \boldsymbol{F} \tag{4}$$

where $\boldsymbol{U}$, the complex-valued vector of nodal displacements, is computed directly from (4). In this case, hysteretic (structural) damping can be conveniently assumed for the harmonic solution, reducing (4) to

$$\left(-\omega^2\boldsymbol{M} + \boldsymbol{K}(1 + i\eta)\right)\boldsymbol{U} = \boldsymbol{F} \tag{5}$$

where η is the ratio between the energy dissipated during one loading cycle to the maximum potential (elastic) energy given by

$$\eta = \frac{E_{d,per\ cycle}}{2\pi E_{p,max}} \tag{6}$$

For the simulations associated with the steady-state vibrations (time-harmonic simulations), the hysteretic damping coefficient of $\eta = 0.05$ was used. For the numerical simulations associated with the hammer impact analysis (time-dependent transient simulations), two sets of Rayleigh damping coefficients were chosen. The first set provides consistency between both time-harmonic and transient

damping models by setting $\alpha = \frac{\eta}{\overline{\omega}} = 1.277 \times 10^{-4} s$ and $\mu = 0$, whereas the second set assumes $\alpha = 5 \times 10^{-5} s$, and $\mu = 5 \times 10^{-5} s^{-1}$. The value $\frac{1}{\overline{\omega}}$ is computed using the integral average between the lower and upper bound of radial frequencies used for the time-independent harmonic simulations: $\omega_{lb} = 188.5 \, rad/s$, $\omega_{ub} = 722.6 \, rad/s$.

$$\frac{1}{\overline{\omega}} = \frac{1}{\omega_{ub} - \omega_{lb}} \int_{\omega_{lb}}^{\omega_{ub}} \frac{1}{\omega} d\omega \tag{7}$$

It is emphasized that two damping models are inserted into the FEA model, and thus into the machine learning framework, to cater to field simulations where soil damping is inherently variable and largely unknown.

3.2 FEA MODEL: HMLT FOUNDATION AND SENSING SETUP

Figure 3.1 illustrates a model of the foundation geometry and corresponding finite element mesh with the SCP observation line near the foundation pile(s). The small circle shown beneath the y-axis line, on top of the pile cap, is the "point" of excitation for the numerical modeling. For the analysis, linear tetrahedral elements were chosen with the minimum number of elements per wavelength set at 8. Absorbing boundary elements [6] were used on the model's *outer boundary of the soil region*, to absorb the outgoing visco-elastodynamic wave and so mimic the infinite soil domain. For completeness, Fig. 3.1 also illustrates the mesh of a complete FEA model that includes both the foundation and surrounding soil region.
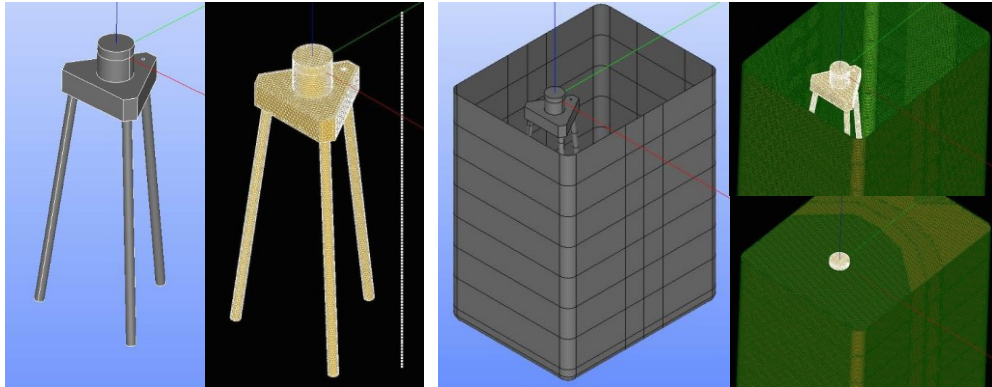
Figure 3.1 T-100 tower foundation; left = foundation model and finite element mesh; right = foundation model with outer soil boundary including mesh of absorbing boundary elements and total soil domain.

The results, in terms of displacement amplitudes or time histories, from each numerical simulation were recorded at various distances and orientations relative to the pile cap to gain a better understanding of the overall waveform generated in the soil region surrounding the pile of interest. As an example, Fig. 3.2 shows a foundation model with "sample" SCP observation lines (indicated in red). Motivated by the limitations of SCP testing conditions, the distance from the center of the tower to the SCP observation line is allowed to vary from 3.6 m to 6.5 m. Additionally, the azimuthal offset orientations of the observation lines were set at 0°, 15°, and 30° from the pile's orientation. The placement of multiple SCP

observation paths in the vicinity of the pile was designed to produce ten SCP datasets (i.e. vertical displacement profiles) for the vibration method, and nine SCP datasets for the hammer impact method, per simulation. Similar simulations were performed on T-100 and T-120 tower foundation geometries.

In terms of steady-state simulations, the driving frequency was varied between 30 Hz – 55 Hz and 90 Hz – 115 Hz with 5 Hz increments to match the frequency ranges of the two vibratory shakers deemed to be best candidates for field testing. The simulated pile depth for the vibratory method was varied, in 1 m increments, between 3 m – 14 m, while the pile end depth for the hammer impact method varied between 2.5 m – 14.5 m using 0.5 m increments. A finer pile depth increment was conveniently used for the hammer impact analysis since this method foregoes the driving frequency parameter of the vibration analysis, which in turn drastically reduces the number of parametric simulations. Simulations were repeated for the frequency and foundation geometry configurations using varied soil properties and profiles. Two homogenous soil profiles were used, with the second profile having a Young's modulus, E, twice the value of the first profile. Additionally, soil profiles, where the stiffness of the soil was linearly increased with depth, were used. The coverage of these multiple parameters and foundation geometries allowed for a sizeable number of simulations, providing thousands of ML training data points for the two NDE methods. Tables 3.1 – 3.5 list the soil profiles and material properties used for the vibration and hammer impact analysis modeling, including the number of simulations performed for each soil profile and method.

Table 3.1 Vibration analysis soil profile #1 material properties.

Vibration method soil profile #1: 288 simulations = 2880 synthetic training data points								
Depth	0 - 2 m	2 - 4 m	4 - 6 m	6 - 8 m	8 - 10 m	10 - 12 m	12 - 14 m	14 - 15 m
E [MPa]	40	40	40	40	40	40	40	40
ρ [kg/m³]	1840	1840	1840	1840	1840	1840	1840	1840
ν [ ]	1/3	1/3	1/3	1/3	1/3	1/3	1/3	1/3
Vs [m/s]	90.3	90.3	90.3	90.3	90.3	90.3	90.3	90.3

Table 3.2 Vibration analysis soil profile #2 material properties.

Vibration method soil profile #2: 288 simulations = 2880 synthetic training data points								
Depth	0 - 2 m	2 - 4 m	4 - 6 m	6 - 8 m	8 - 10 m	10 - 12 m	12 - 14 m	14 - 15 m
E [MPa]	20	40	60	80	100	120	140	160
ρ [kg/m³]	1850	1850	1850	1850	1850	1850	1850	1850
ν [ ]	1/3	1/3	1/3	1/3	1/3	1/3	1/3	1/3
Vs [m/s]	63.7	90.0	110.3	127.3	142.4	156.0	168.5	180.1

Table 3.3 Hammer impact analysis soil profile #1 material properties.

Hammer impact method soil profile #1: 100 simulations = 900 synthetic training data points								
Depth	0 - 2 m	2 - 4 m	4 - 6 m	6 - 8 m	8 - 10 m	10 - 12 m	12 - 14 m	14 - 15 m
E [MPa]	40	40	40	40	40	40	40	40
ρ [kg/m³]	1840	1840	1840	1840	1840	1840	1840	1840
ν [ ]	1/3	1/3	1/3	1/3	1/3	1/3	1/3	1/3
Vs [m/s]	90.3	90.3	90.3	90.3	90.3	90.3	90.3	90.3

Table 3.4 Hammer impact analysis soil profile #2 material properties.

Hammer impact method soil profile #2: 100 simulations = 900 synthetic training data points								
Depth	0 - 2 m	2 - 4 m	4 - 6 m	6 - 8 m	8 - 10 m	10 - 12 m	12 - 14 m	14 - 15 m
E [MPa]	80	80	80	80	80	80	80	80
ρ [kg/m³]	1840	1840	1840	1840	1840	1840	1840	1840
ν [ ]	1/3	1/3	1/3	1/3	1/3	1/3	1/3	1/3
Vs [m/s]	127.7	127.7	127.7	127.7	127.7	127.7	127.7	127.7

Table 3.5 Hammer impact analysis soil profile #3 material properties.

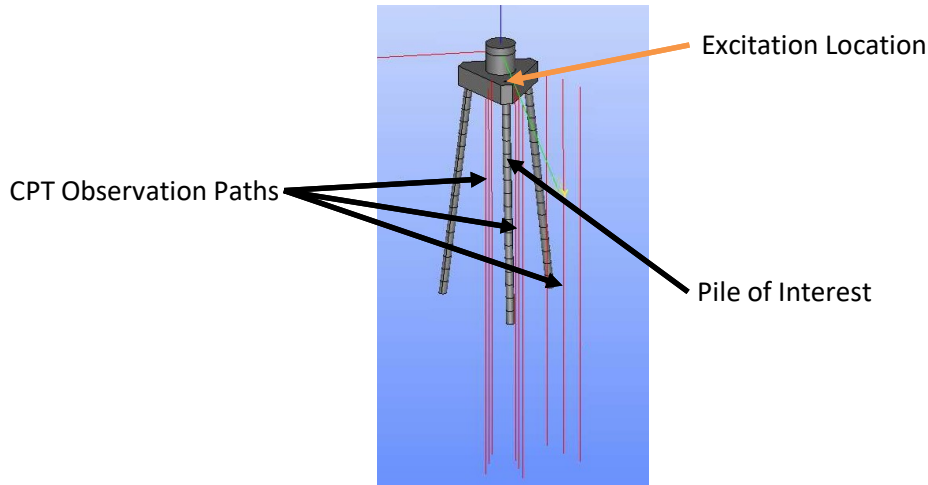| Hammer impact method soil profile #3: 50 simulations = 450 synthetic training data points								
Depth	0 - 2 m	2 - 4 m	4 - 6 m	6 - 8 m	8 - 10 m	10 - 12 m	12 - 14 m	14 - 15 m
E [MPa]	40	50	60	70	80	90	100	110
ρ [kg/m³]	1840	1840	1840	1840	1840	1840	1840	1840
ν [ ]	1/3	1/3	1/3	1/3	1/3	1/3	1/3	1/3
Vs [m/s]	90.3	100.9	110.6	119.4	127.7	135.4	142.8	149.7

Figure 3.2 HMLT foundation model geometry with CPT observation field.

3.3 NUMERICAL RESULTS

3.3.1 Steady-State Vibration Analysis

Concerning the time-harmonic analysis, our focus is on the magnitude $\|\boldsymbol{v}\| = \left(v_x \overline{v_x} + v_y \overline{v_y} + v_z \overline{v_z}\right)^{1/2}$ of the complex-valued particle velocity vector along the SCP sensing line. To illustrate the FEA simulations, the left panel in Fig. 3.3 shows the norms of the real part ($\|\mathrm{Re}(\boldsymbol{v})\|$) and imaginary part ($\|\mathrm{Im}(\boldsymbol{v})\|$) of the particle velocity vector in the plane containing the axis of the tower and the SCP sensing line, with the latter indicated in yellow. For completeness, the right panel in Fig. 3.3 illustrates the *profile of $\|\boldsymbol{v}\|$ versus sensing depth*, which is taken as *the input for inverse analysis*. In the panel, the blue horizontal dashed line indicates the depth of where the pile terminates, 6.75 m deep for this example.
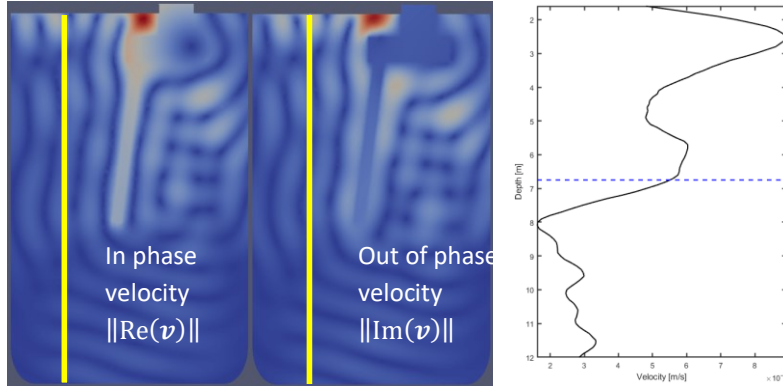
Figure 3.3 Steady state visco-elastodynamic response; left = real and imaginary vector fields, right = ground velocity magnitude along observation path.

Once computed, the numerical results of the overall ground motion are normalized, in a similar fashion as Eq. (2),

$$\bar{V} = \frac{V}{\sqrt{V^T V}}, \qquad \|\bar{V}\|_2 = 1, \tag{8}$$

so that the L2-norm of the ground motion vector is unity. In this setting, Fig. 3.4 shows $\bar{V}$, i.e. the normalized ground response, for three different pile end depths at a 50 Hz driving force. Fig. 3.5 shows the same comparison, but for a driving force of 100 Hz. Again, the horizontal dashed lines indicate the pile end depth in the FEA model.
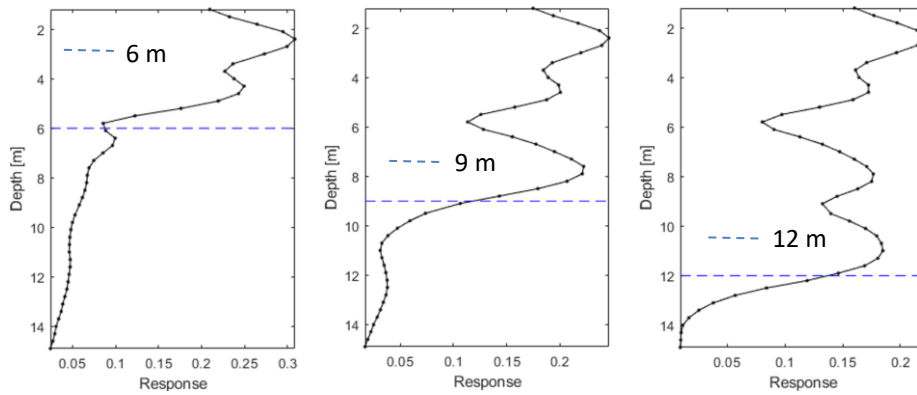

Figure 3.4 Steady-state simulations; 50 Hz excitation, normalized velocity magnitude profile collected in $\bar{V}$.
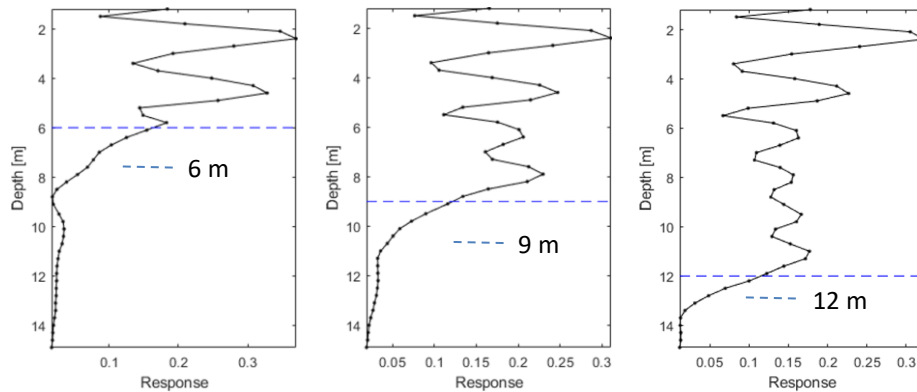

Figure 3.5 Steady-state simulations; 100 Hz excitation, normalized velocity magnitude profile collected in $\bar{V}$.

14

3.3.2 Hammer Impact Analysis

For the hammer impact analysis, the wavelet function shown in Fig. 3.6 was used to simulate the vertical impact force applied to the pile cap. A low frequency content, representing the anticipated field testing conditions, is the primary reason behind this wavelet selection.
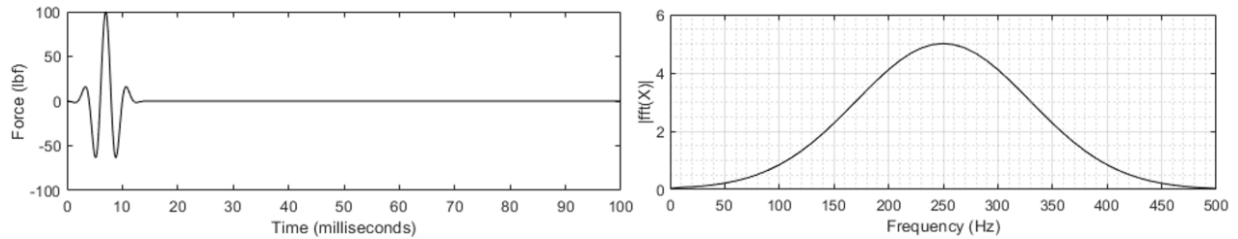

Figure 3.6 Wavelet function of simulated hammer impact; time domain variation (left) and Fourier amplitude spectrum (right).

To illustrate the temporal signature of the ground motion stemming from FEA simulations, Fig. 3.7 shows the "waterfall plot" of transient responses (along the SCP sensing line) in terms of $v(z_j, t)$, where the vertical axis is the sensing depth and the horizontal axis represents time. In the display, the respective pile ends (at 6 m, 9 m, and 12 m) featured by the FEA model are indicated with horizontal dashed lines.
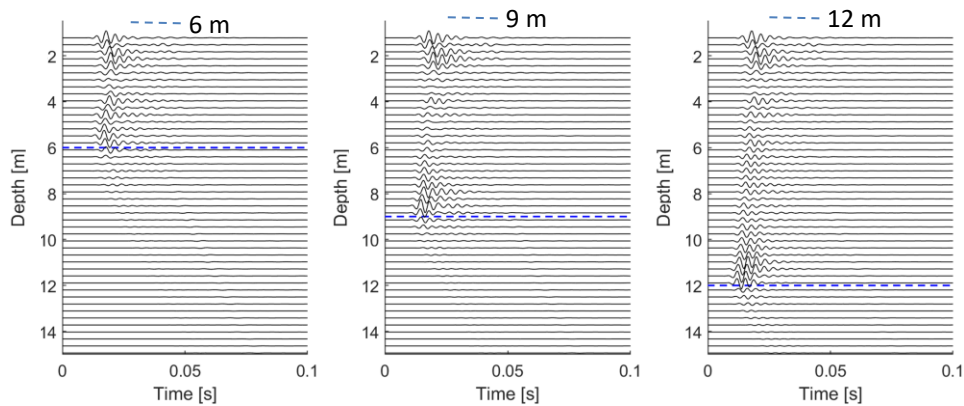

Figure 3.7 Hammer impact simulations; waterfall plots of the arrival times along CPT sensing line.

CHAPTER 4: ML-BASED INVERSE SOLUTION

4.1 ARCHITECTURE OF A DEEP NEURAL NETWORK

In what follows, deep neural networks are designed to synthesize the causal relationship between the pile depth (assumed by the FEA model) and the ground motion profiles along the SCP sensing line (the output of FEA simulations) for both: (i) steady-state, and (ii) hammer-impact testing configurations. In principle, neural networks use a training approach based on iterative optimization to develop a network of weights, biases, and non-linear activation functions to predict a single output value (regression network) or a set of output values (classification network). Figure 4.1 displays the configuration of a regression neural network with two hidden layers. The number of hidden layers, as well as the depth of each layer (denoted by indices q and p in the figure), are all hyper-parameters of the network that are user specified. The length of the input vector of the i-th training example, $X^{[i]}$, is denoted as n. In general, neural networks with two or more hidden layers are classified as deep neural networks.
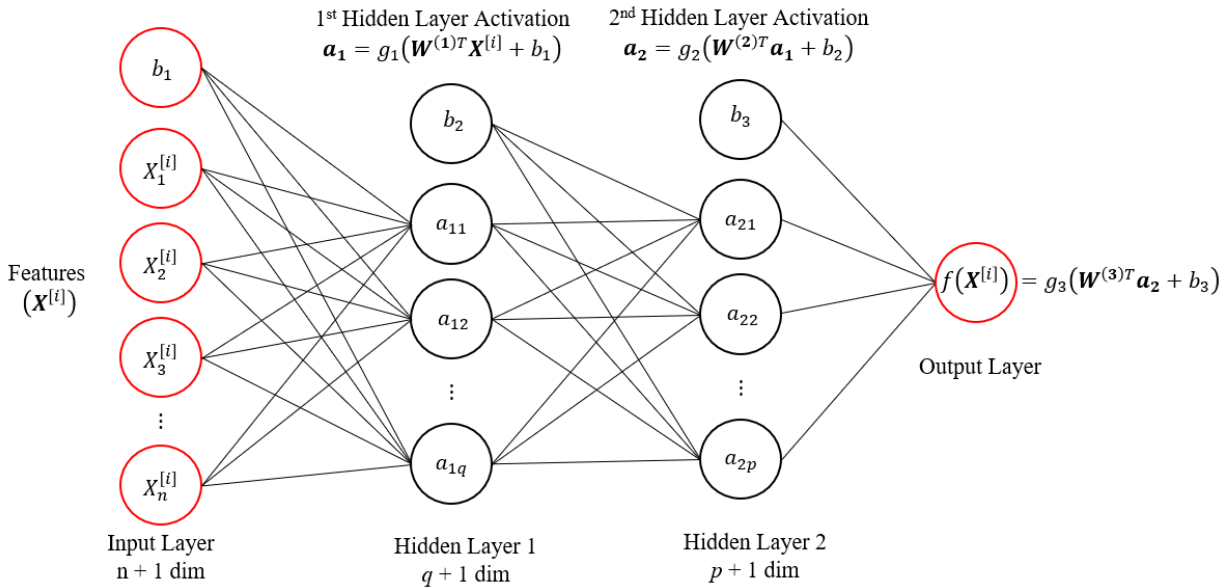

Figure 4.1 Architecture of a neural network with two hidden layers.

In the display, $g_i(Z)$ signifies a non-linear activation function, typically a Sigmoid function: $g(Z) = \frac{1}{1+e^{-Z}}$, ReLU (Rectified Linear Unit): $g(Z) = max(Z, 0)$, or Hyperbolic Tangent function: $g(Z) = \tanh(Z)$.

The network's connection weight matrices $\boldsymbol{W}^{(j)}$ and bias values b_j (referred to via generic notation $\boldsymbol{W}$ and b), are trained using a set of training examples, $\boldsymbol{X}$, that have known output values, $\boldsymbol{Y}$. A loss function, $J(\boldsymbol{W}, b; \boldsymbol{X}, \boldsymbol{Y})$, provides a measure of the difference between predicted network output values and corresponding target output values. The addition of either L1- or L2-norm weight regularization [7] places a loss factor, λ, on the magnitude of the weights to prevent the network from overfitting the training data and underperforming on the validation data. The regularization term λ increases the value of the loss function proportional to the size of the algorithm's weights; therefore, the training algorithm will try to fit the training data while keeping the size of the weights at a minimum.

A process known as backpropagation uses the partial derivatives of the loss function with respect to the network's parameters, W and b, to update the weights and biases at each training step as the network "learns" the training data [8]. Equation (9) shows the least squares regression loss function with L2-norm weight regularization used to train the network for both the steady-state and hammer impact analysis.

$$J(W, b; X, Y) = \frac{1}{m} \sum_{i=1}^{m} \left(f(X^{[i]}) - Y^{[i]}\right)^2 + \frac{\lambda}{2m} \sum_{l=1}^{L-1} \sum_{k=1}^{s_l} \sum_{j=1}^{s_{l+1}} \left(W_{kj}^{(l)}\right)^2 \tag{9}$$

In (9), m is the number of training examples in each mini batch (a random split of the training data for a backpropagation parameter update), λ is the weight regularization value, L is the number of layers (including input and output layers), s_l is the size of layer l, and s_{l+1} is the size of layer $l + 1$.

Keras, a deep learning application programming interface (API) written in Python and running on top of the ML platform *TensorFlow* [9, 10], is used to build and run the neural networks for the synthetic numerical data. An example code used to generate a typical neural network using *Keras* and *TensorFlow* framework is shown in Fig. 4.2.

```python
import tensorflow
from tensorflow.keras import models
from tensorflow.keras import layers
from tensorflow.keras import optimizers


lam = 0.0175
network = models.Sequential()

network.add(layers.Dense(50,activation='relu',input_shape=(nn,),
                         kernel_regularizer=tensorflow.keras.regularizers.l2(l=lam)))

network.add(layers.Dense(25,activation='relu',
                         kernel_regularizer=tensorflow.keras.regularizers.l2(l=lam)))

network.add(layers.Dense(20,activation='relu',
                         kernel_regularizer=tensorflow.keras.regularizers.l2(l=lam)))

network.add(layers.Dense(1))

network.compile(optimizer=optimizers.Adam(learning_rate=0.0005),
                loss='mse',metrics=['mae'])

history=network.fit(X_train,y_train,epochs=3000,batch_size=256,
                    validation_data=(X_test,y_test),verbose = 2)
```

Figure 4.2 Neural network development using *Keras*, written in Python language.

From the example code in Fig. 4.2, it can be seen that $\lambda = 0.0175$ for the L2-norm weight regularization. The network has three hidden layers with sizes of 50, 25, and 20. The output layer has a size of one. The gradient descent backpropagation uses the Adam optimizer [11] with learning rate of 0.0005. The training data is split into mini batches with size of 256 and trains the network for 3000 epochs (or 3000 loops over the entire training data set). In the call to fit the network, the test data (data held apart from the network training data) are used to validate the fit of the network on every training iteration update. A plot of the training and validation loss evolution gives good insight on the performance of the network during training.

4.2 PERFORMANCE OF THE NEURAL NETWORK

4.2.1 Steady-State Vibration Analysis

For the numerical simulations performed using the steady-state vibration analysis, the input into the neural network is the unit-norm vertical profile of the ground motion magnitude, $\overline{V}$, introduced in Sections 2.1 and 3.3.1. Figure 4.3 displays an example set of pile depth predictions on data from the *test group* compared to the actual (synthetic) pile depth. Figure 4.4 shows the residual error values (predicted pile depth – actual pile depth) for both the training and test groups, including the evolution of the loss and mean absolute error values during training. For the test group of steady-state simulations, the root mean squared error (RMSE) is 0.812, and the R^2 goodness of fit is 0.964.
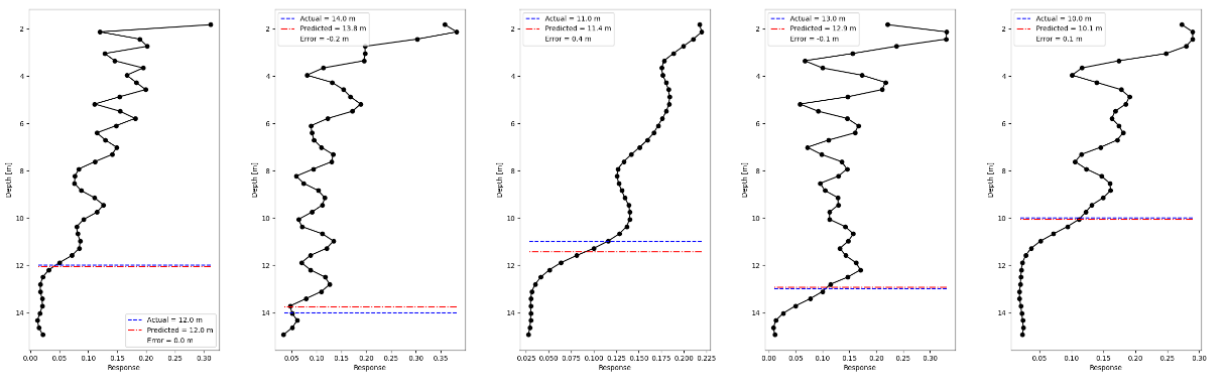

Figure 4.3 Example predictions of "in situ" pile depth from the vibratory analysis test data set.
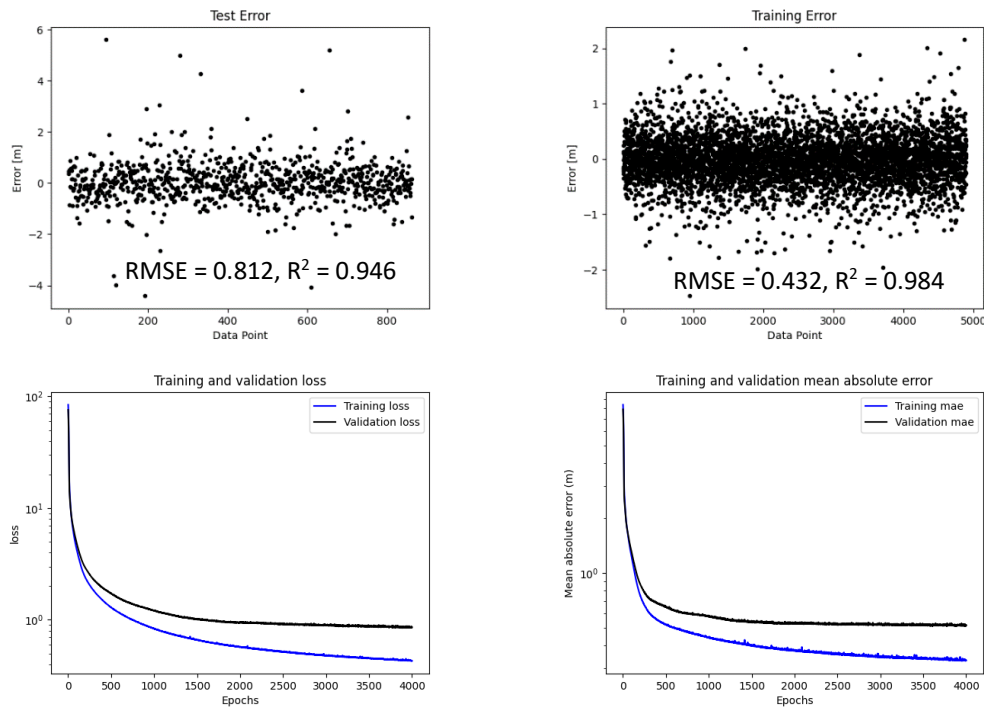

Figure 4.4 Network training metrics for the steady-state vibration analysis; upper left = testing error, upper right = training error, bottom left = evolution of the loss value, bottom right = evolution of the mean absolute error.

4.2.2 Hammer Impact Analysis

To train the network for the hammer impact analysis simulation data, the time traces from the cascading plots shown in section 3.3.2 were unrolled to form a single feature vector as input for the ML algorithm. Figures 4.5 and 4.6 show example prediction outputs and network training metrics for the hammer impact analysis that are analogous to their steady-state predecessors. For the hammer impact analysis test group, the RMSE is 0.322, and the R^2 goodness of fit is 0.992.
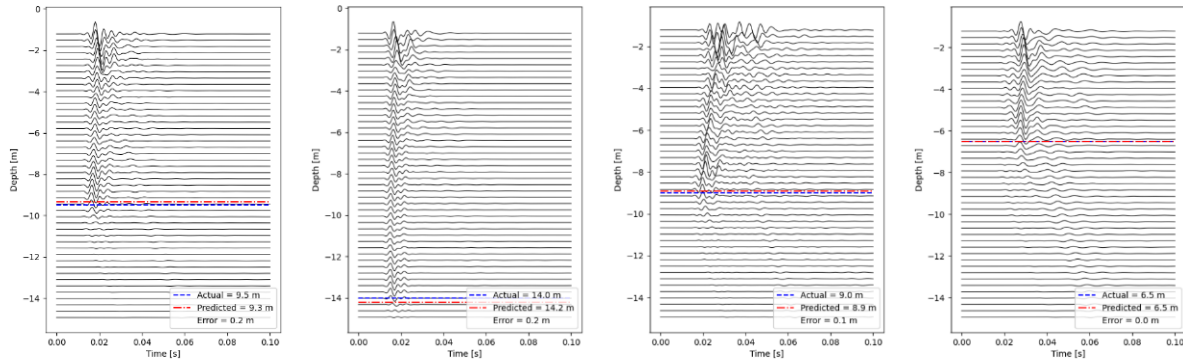

Figure 4.5 Example predictions of "in situ" pile depth from the hammer impact analysis test data set.
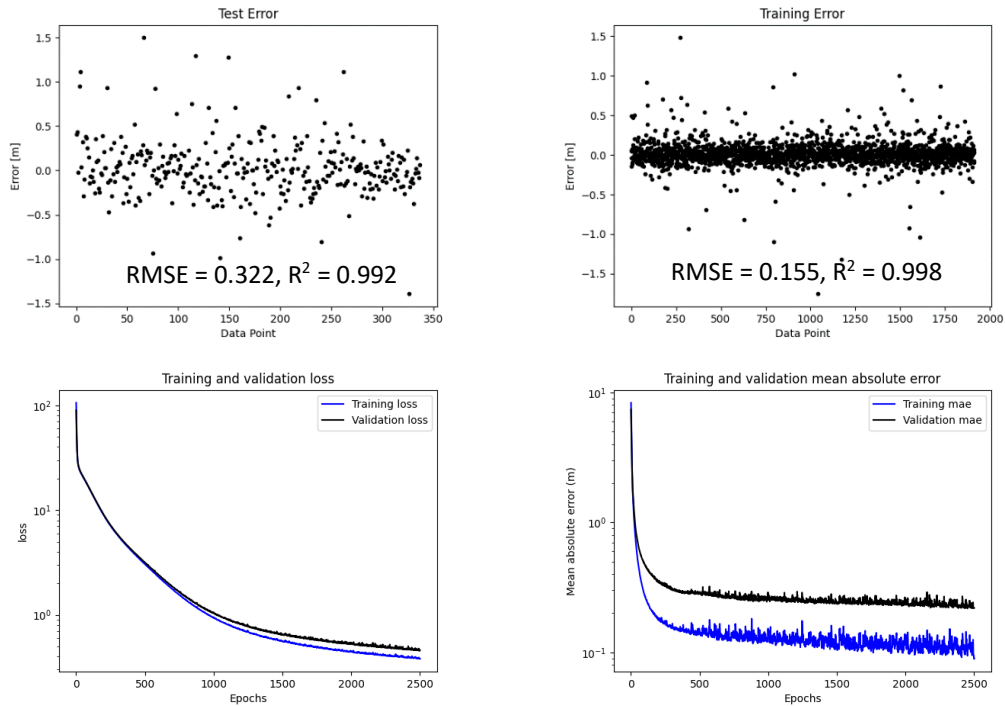

Figure 4.6 Network training metrics for the hammer impact analysis; upper left = testing error, upper right = training error, bottom left = evolution of the loss value, bottom right = evolution of the mean absolute error.

CHAPTER 5: HMLT FIELD TESTING

Nondestructive testing of HMLT foundation systems was performed between September 2020 and June 2022 at four tower sites in the Twin Cities metro area: Mendota Heights, Burnsville, Shakopee, and Eden Prairie Minnesota. The induced ground motion from both vibratory shaker and hammer impact methods is recorded at increasing depths using a SCP geophone. During the field testing, it was demonstrated that both testing methods can be implemented side-by-side, using the same metal rod and mounting plate combination in contact with the top of the pile cap, allowing for two measurements – vibratory shaker and impact – at each elevation (i.e. depth) of the SCP geophone. The testing depths were from 4 ft – 49 ft (1.2 m – 14.9 m), at 1 ft increments.

5.1 PRELIMINARY INVESTIGATION PROCEDURE

Previous tower investigations have shown that, contrary to initial expectations, there are no in-ground pile cap orientation identifiers on the above ground portion of the tower's foundation. Figure 5.1 displays the in-ground pile cap geometry, including the portion of the foundation that is visible above ground.
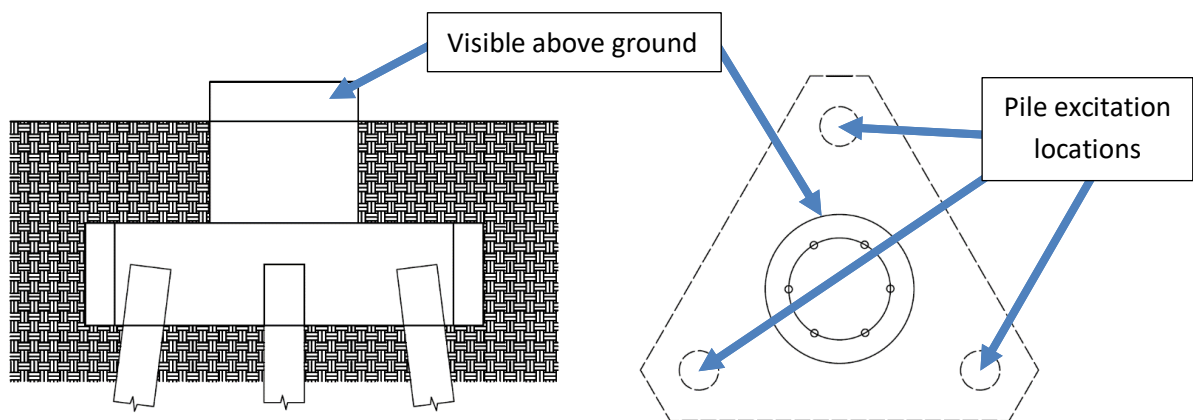

Figure 5.1 Cross-section view (left) and plan view (right) of in-ground pile cap.

As seen in Fig. 5.1, the optimal pile excitation locations are on top of the pile cap, directly above the pile. Testing performed at other positions has shown a loss of efficiency and increased background noise due to excessive pile cap vibrations when the excitation is not located directly over the pile.

A preliminary investigation procedure, using a handheld soil probe and ground marking paint, was developed to proactively determine the pile cap geometry and orientation. The investigation procedure involves pushing the soil probe into the soil in the vicinity of the base of the tower to contact the concrete pile cap. Once the edge of the pile cap is determined, the ground is marked by paint in that location. By connecting the paint marks, the geometry and orientation of the semi-triangular foundation pile cap is projected to the surface of the soil. Figure 5.2 shows the preliminary investigation procedure, and the results obtained. To capture the orientation and geometry of the pile cap in a permanent record, the base of the tower is marked with the direction of, and distance to, each pile cap corner. The bottom right image in Fig. 5.2 shows that the edge of the pile cap corner is roughly 78 in. from the side of the base of the

tower. Knowing these details about the pile cap before testing will provide guidance on (i) placing the metal testing rod and (ii) positioning the SCPT truck. The goal of this procedure is to ensure that the testing is performed directly over the pile of interest and that the CPT seismic cone is near the pile (10 ft - 15 ft) while testing.

Figure 5.2 Preliminary investigation results on in-ground pile cap orientation and geometry.

5.2 HMLT FIELD TESTING RESULTS

5.2.1 September 17, 2020: HMLT E3A-11 Mendota Heights, MN

HMLT Pole ID: E3A-11 was nondestructively tested on September 17, 2020. Tower E3A-11, a T-120 tower, is in the I-494 / I-35E interchange in Mendota Heights, MN. A single pile was evaluated during field testing at the Mendota Heights location with a single CPT push. Figure 5.3 shows the location of HMLT E3A-11 and the positions of the tested pile.
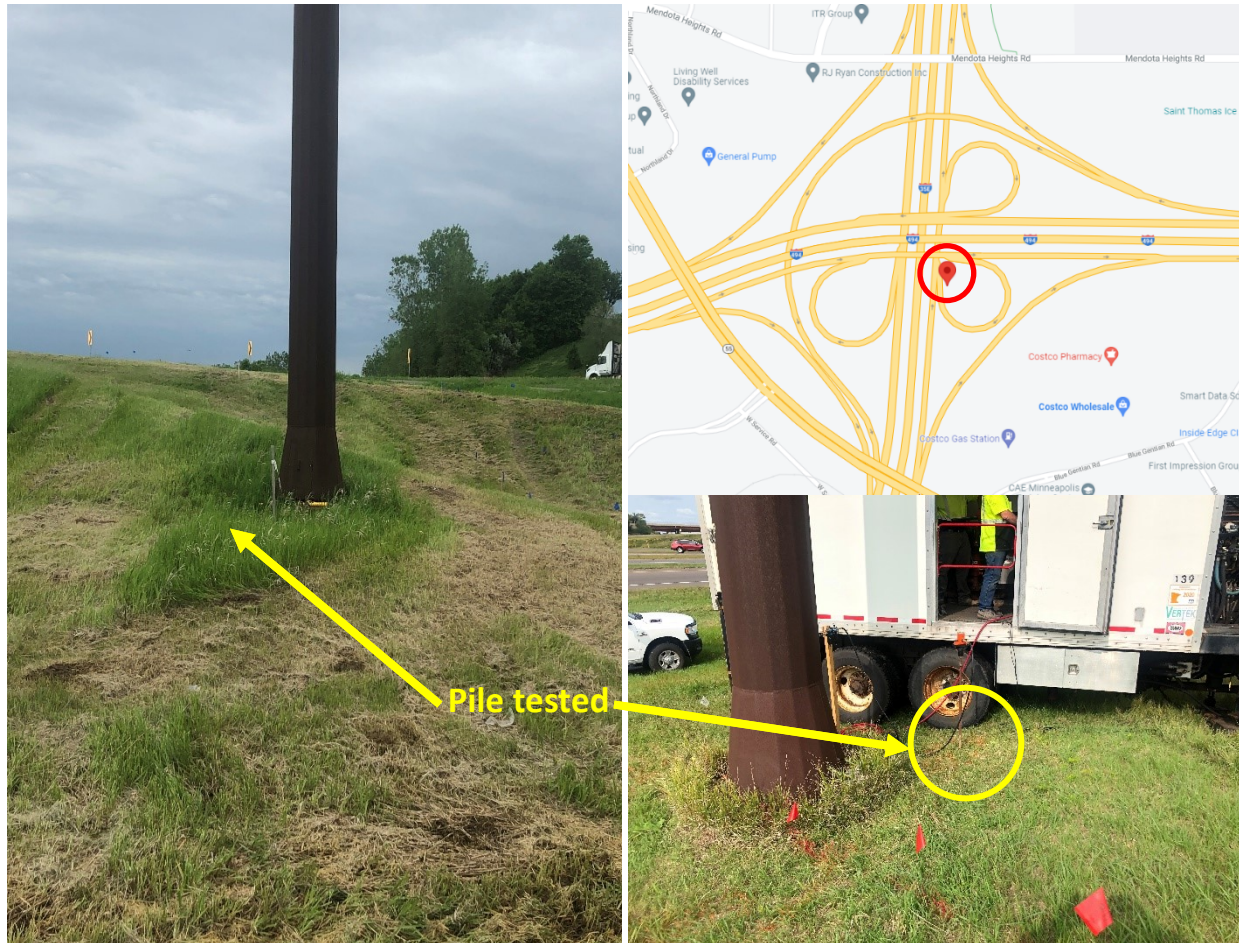

Figure 5.3 HMLT E3A-11 location and pile tested.

The pile was evaluated with both the hammer impact and vibratory shaker (low frequency shaker, 55 Hz) tests. The higher frequency shaker was tried on tower E3A-11, but the metal rod in contact with the top of the pile cap repeatedly bounced off the pile cap due to the higher frequency. This has been remedied by the addition of weights to the metal rod to keep it in contact with the pile cap. The added weights can be seen in Figures 2.6, 5.6, and 5.10. There is no recorded pile length for tower E3A-11 in the MnDOT 'High Mast Light Tower database MDH' file. The results of the field tests on tower E3A-11, including neural network predicted depth outputs, are shown in Figure 5.4. In the figure, the maroon dotted lines are outputs from thirty inputs into the neural network, with the solid red line as the averaged predicted depth.
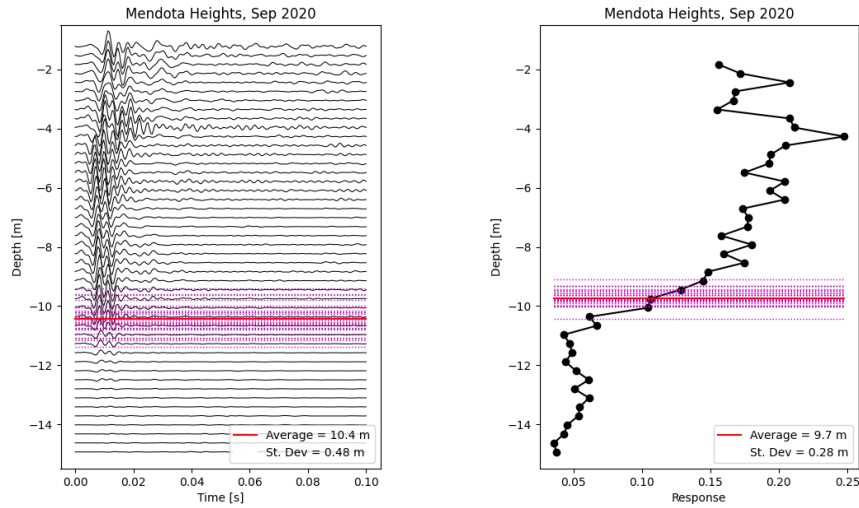
Figure 5.4 HMLT E3A-11 field-test results: left = hammer impact, right = vibratory shaker.

During the HMLT foundation testing, soil stratigraphy information was collected with the CPT rig. Two standard CPT tests (CT1 and CT2) were performed at the tower site. Figure 5.5 shows the soil stratigraphy at the tower foundation. The predominant soil is clean sand, soil behavior type (SBT) 6, with a layer of SBT 3 – 5, sand/silt/clay mixture, from depths 5 – 15 ft. The soil is uniform clean sand at depths greater than 15 ft. The pore pressure results show that there was no groundwater encountered during the testing.
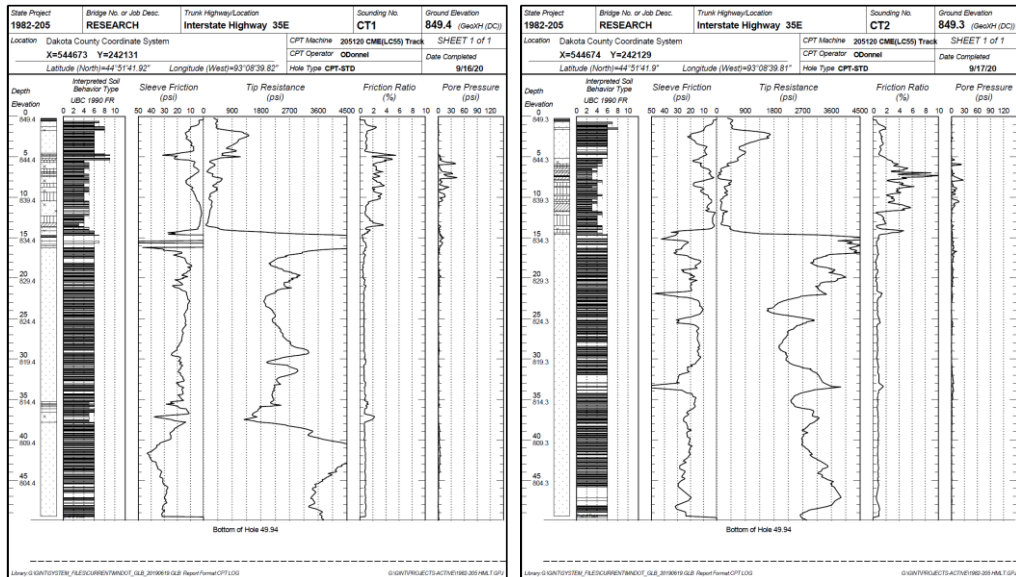

Figure 5.5 CPT results at HMLT E3A-11; left = Sounding CT1, right = Sounding CT2.

The deeper results (> 15 ft) from the CPT show that the foundation's piles are in uniform clean sand to silty sand. This indicates that the change in ground motion response observed in both testing methods is most likely due to the end of the pile, not a change in foundation soil or material stiffness.

5.2.2 September 13 & 14, 2021: HMLT W1L-5 Burnsville, MN

HMLT Pole ID: W1L-5 was nondestructively tested on September 13 and 14, 2021. Tower W1L-5, a T-120 tower, is in the I-35W / TH 13 interchange in Burnsville, MN. A single pile was evaluated during field testing at the Burnsville location, however, the pile, which points to the north, was evaluated twice with two separate CPT pushes. Figure 5.6 shows the location of HMLT W1L-5 and the position of the tested pile.
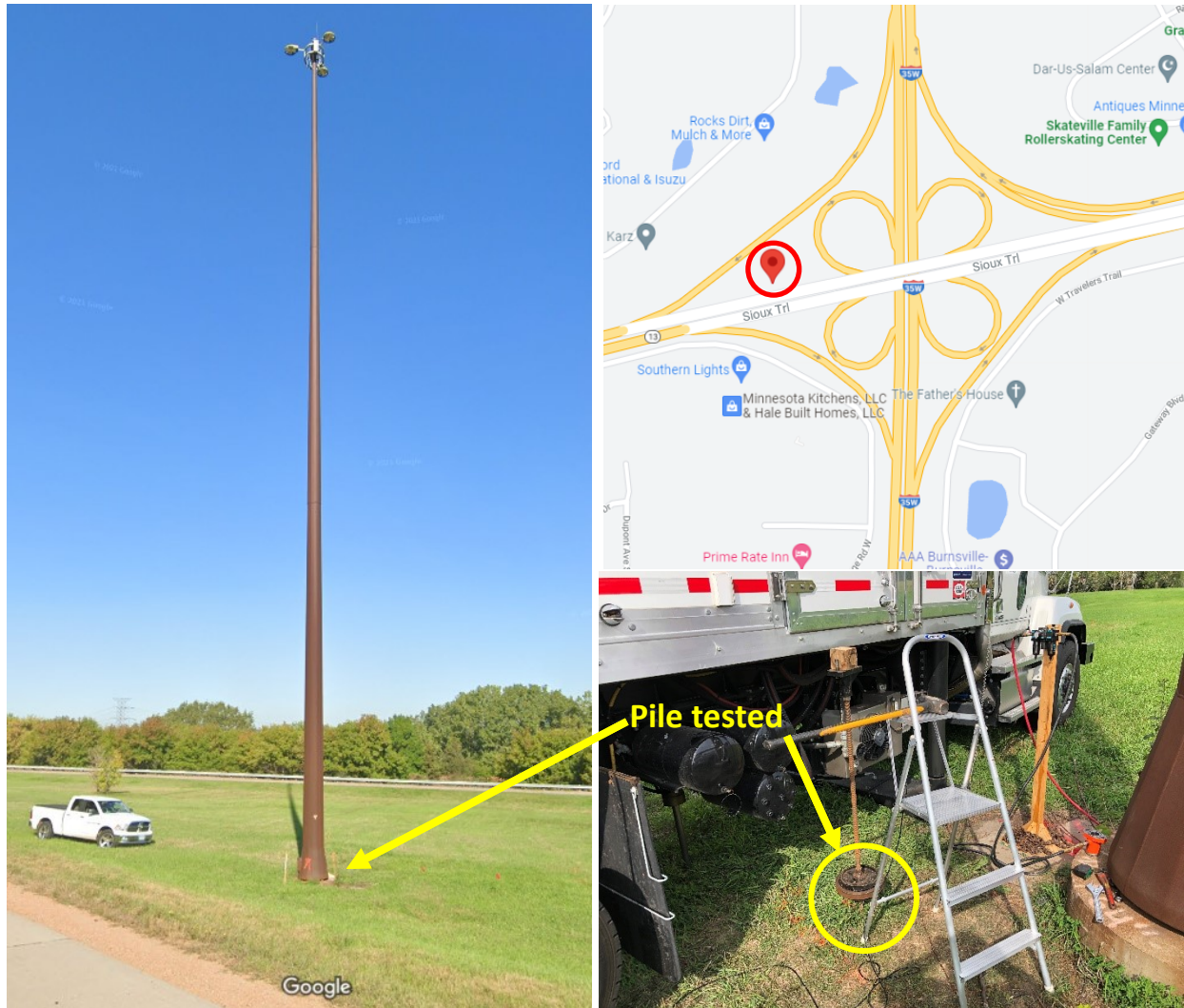

Figure 5.6 HMLT W1L-5 location and pile tested.

The pile was evaluated with both the hammer impact and vibratory shaker (both frequency shakers, 55 Hz and 85 Hz) tests. The higher frequency shaker was only used during the second day of testing, providing only one set of data corresponding to the high frequency shaker. The 'High Mast Light Tower database MDH' excel file shows recorded pile length of 20 ft (6.1 m) for tower W1L-5. During testing, there was 20 inches of soil from the ground surface to the top of the pile cap, additionally, typical details show 1.5 ft of concrete between the top of the pile cap and the uppermost insertion point of the pile. Accounting for this distance from the ground surface to the top of the pile, and the pile's inclination of 7.125°, this gives an expected pile embedment depth of 23 ft (7m). The field-testing results for both CPT tests are shown in

Figures 5.7 and 5.8, with expected pile end depth (based on tower database and pile cap geometry information) highlighted as a blue dashed line; dotted maroon and solid red lines indicate the neural network outputs, similar to section 5.2.1.
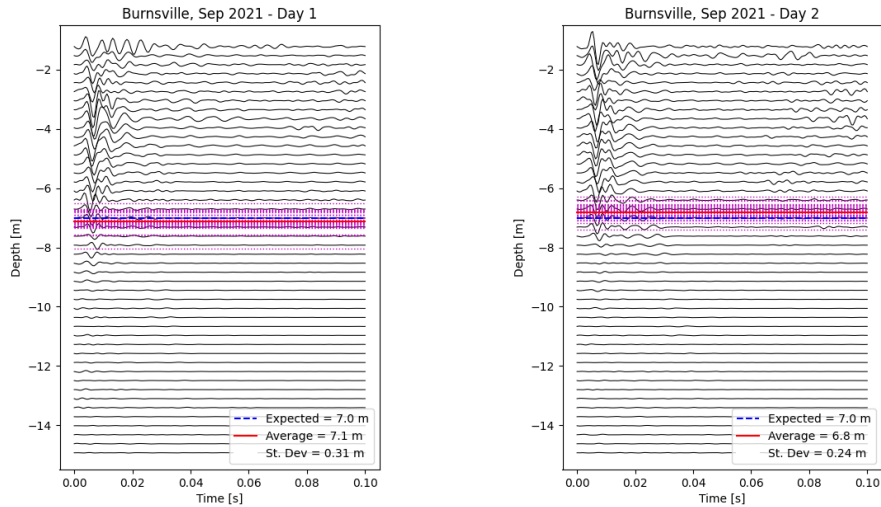

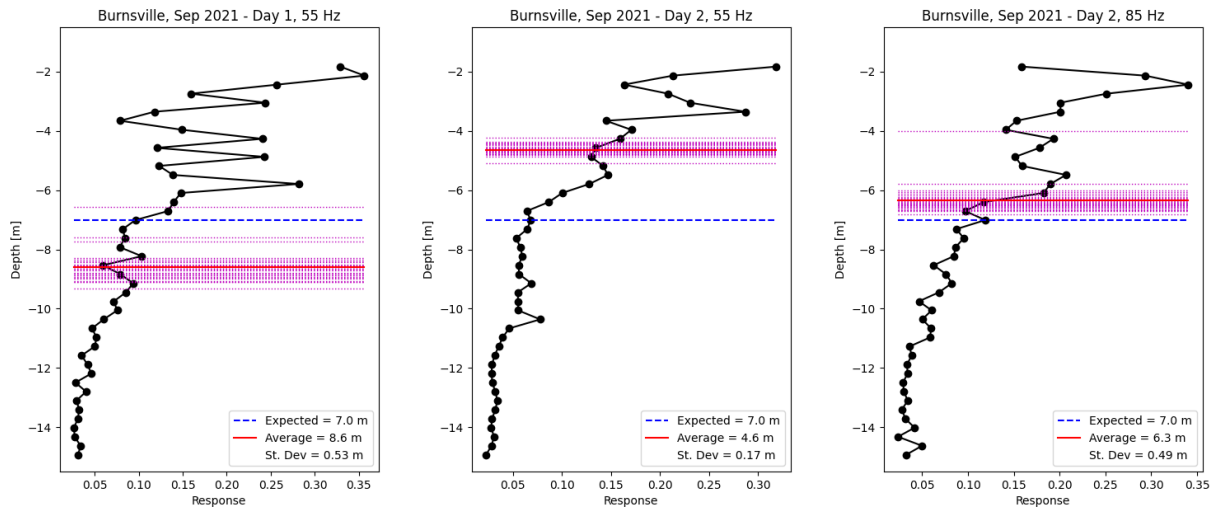Figure 5.7 HMLT W1L-5 hammer impact results; left = day 1, right = day 2.


Figure 5.8 HMLT W1L-5 vibratory shaker results; left = day 1 (lower frequency, 55 Hz), middle = day 2 (lower frequency, 55 Hz), right = day 2 (higher frequency, 85 Hz).

Soil stratigraphy information for the HMLT W1L-5 site was collected via CPT rig in 2005 and 2014. Three standard CPT tests (c009, S01, and S02) were performed at the tower site. Figure 5.9 shows the location of the CPT investigations and the soil stratigraphy at the tower foundation. The predominant soil type from the ground surface to a depth of $15\,\text{ft} - 20\,\text{ft}$ is SBT $6 - 8$, clean to stiff sand with gravel, and at depths deeper than 20 ft the SBT is $4 - 5$, sand and silt mixtures. The pore pressure results show that there was no groundwater encountered during the testing.

The following soil behavior type classification is used:
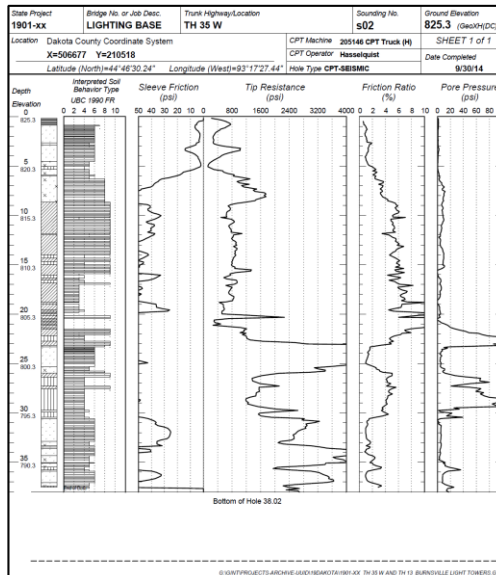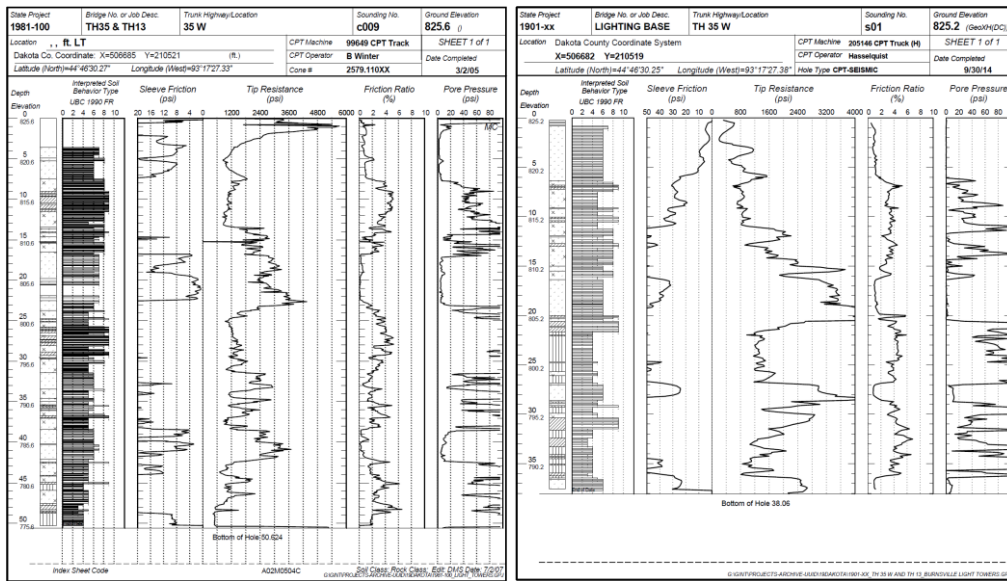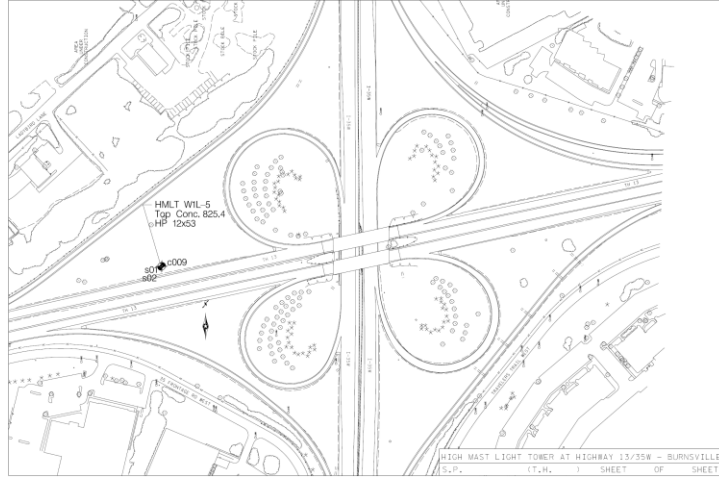
1. Sensitive, Fine Grained
2. Organic Soils - Peats
3. Clays - Clay to Silty Clay
4. Silt Mixtures - Clayey Silt to Silty Clay
5. Sand Mixtures - Silty Sand to Sandy Silt
6. Sands - Clean Sand to Silty Sand
7. Gravelly Sand to Sand
8. Very Stiff Sand to Clayey Sand
9. Very Stiff, Fine Grained

Figure 5.9 Previous CPT results at HMLT W1L-5; top = CPT locations, middle left = c009, middle right = S01, bottom = S02.

HMLT Pole ID: R19J-7 was nondestructively tested on November 22 & 23, 2021 and May 31, 2022. Tower R19J-7, a T-120 tower, is in the TH 169 / TH 101 interchange in Shakopee, MN. Two piles were evaluated during field testing at the Shakopee location. Pile #1 is pointing in the west-northwest direction and Pile #2 is pointing to the north. Figure 5.10 shows the location of HMLT R19J-7 and the positions of the tested piles.
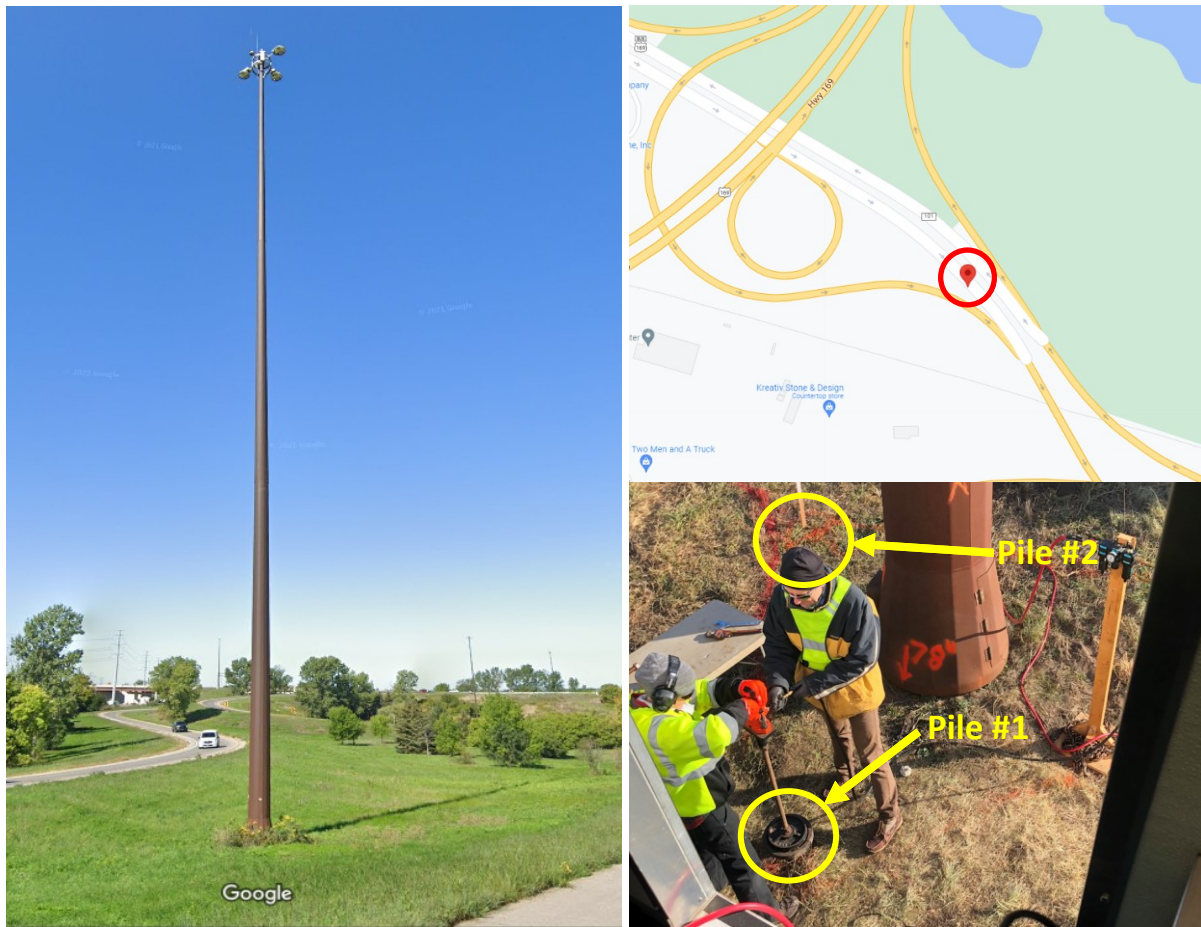

Figure 5.10 HMLT R19J-7 location and piles tested.

The two piles were evaluated with both the hammer impact and vibratory shaker (low frequency shaker, 55 Hz) tests. The higher frequency shaker (85 Hz) had a broken spring while testing Pile #1 and was not in use. The 'High Mast Light Tower database MDH' excel file, provided by MnDOT, shows recorded pile length of 40.8 ft (12.4 m) for tower R19J-7. There was 2.5 ft of soil between the ground surface and top of the pile cap during testing. Again, including the 1.5 ft of concrete pile cap above the pile's uppermost insertion point and the 7.125° inclination of the pile, this gives an estimated pile embedment depth of 44.5 ft (13.6 m). The field-testing results for Piles #1 and #2 are shown in Figures 5.11 and 5.12. In both figures, the estimated pile depth (based on tower database and pile cap geometry information) is highlighted with a blue dashed line; dotted maroon and solid red lines indicate the neural network outputs, similar to section 5.2.1. Pile #1 was retested in May 2022 to verify the hammer impact results

obtained in Fall 2021. The left and middle images in Fig. 5.11 show similarities in the response and repeatability for the two hammer impact tests of the same pile.
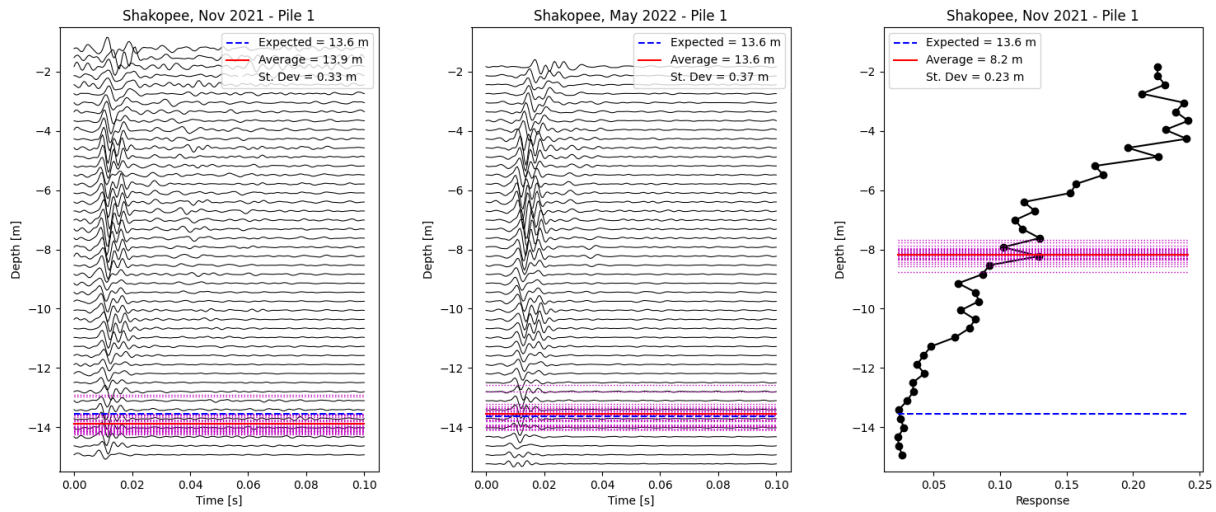

Figure 5.11 HMLT R19J-7 Pile #1 field-test results; left = hammer impact (Nov. 2021), middle = hammer impact (retested May 2022), right = vibratory shaker.
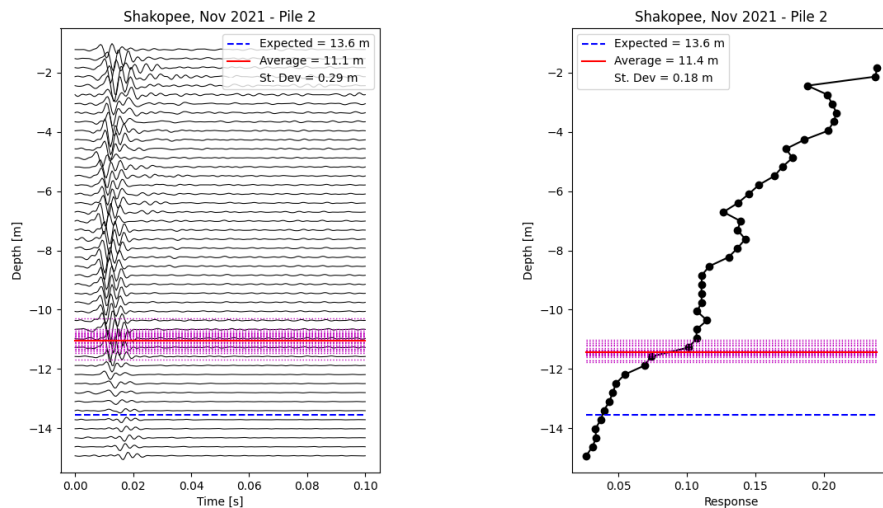

Figure 5.12 HMLT R19J-7 Pile #2 field-test results; left = hammer impact, right = vibratory shaker.

During the HMLT foundation testing in May 2022, soil stratigraphy information was collected with the CPT rig. One standard CPT tests (c100) was performed at the tower site. Figure 5.13 shows the soil stratigraphy at the tower foundation. To a depth of 24 ft the soil is mostly clean sand, soil behavior type 6, with layers of SBT 3 – 6, sand/silt/clay mixture, from depths of 3 ft – 10 ft. From a depth of 24 ft to the bottom of the test there is mostly silty sand mixtures, SBT 5, with a layer of clay, SBT 3, from 30 ft – 35 ft. The pore pressure results show that the groundwater level is at a depth of around 15 ft.
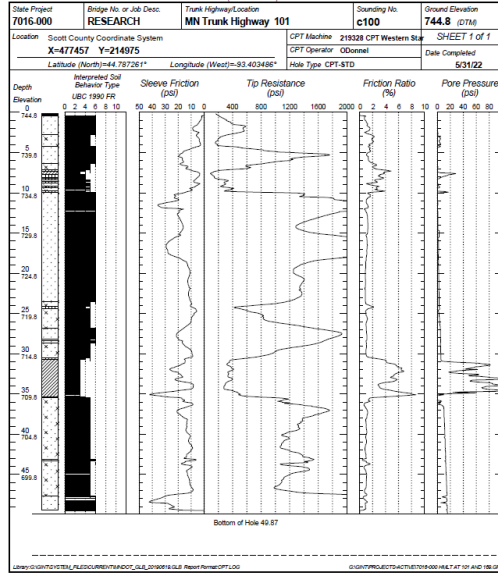
Figure 5.13 c100 CPT results at Tower R19J-7.

29

HMLT Pole ID: S4F-17 was nondestructively tested on June 1, 2022. Tower S4F-17, a T-100 tower, is in the northeastern quadrant of the I-494 / TH 212 interchange in Eden Prairie, MN. Endeavoring to increase overall pile depth testing efficiency and speed, only the hammer impact method of pile depth analysis was implemented at HMLT S4F-17. It was demonstrated that during a single day of HMLT field testing both (i) a traditional CPT soil test was performed and (ii) all three piles of Tower S4F-17 (SE, NE, and W piles) were evaluated using the hammer impact method. Figure 5.14 shows the location of HMLT S4F-17 and images from field testing.

Figure 5.14 HMLT S4F-17 location.

The three piles were evaluated with only the hammer impact method of analysis. The 'High Mast Light Tower database MDH' excel file, provided by MnDOT, shows recorded pile length of 33.1 ft (10.1 m) for HMLT S4F-17. There was 2.5 ft of soil between the ground surface and top of the pile cap during testing. Again, including the 1.5 ft of concrete pile cap above the pile's uppermost insertion point and the 7.125° inclination of the pile, this gives an estimated pile embedment depth of 36.9 ft (11.2 m). The field-testing results for the three piles are shown in Fig. 5.15. In the figure, the estimated pile depth (based on tower database and pile cap geometry information) is highlighted with a blue dashed line; dotted maroon and solid red lines indicate the neural network outputs, similar to section 5.2.1.
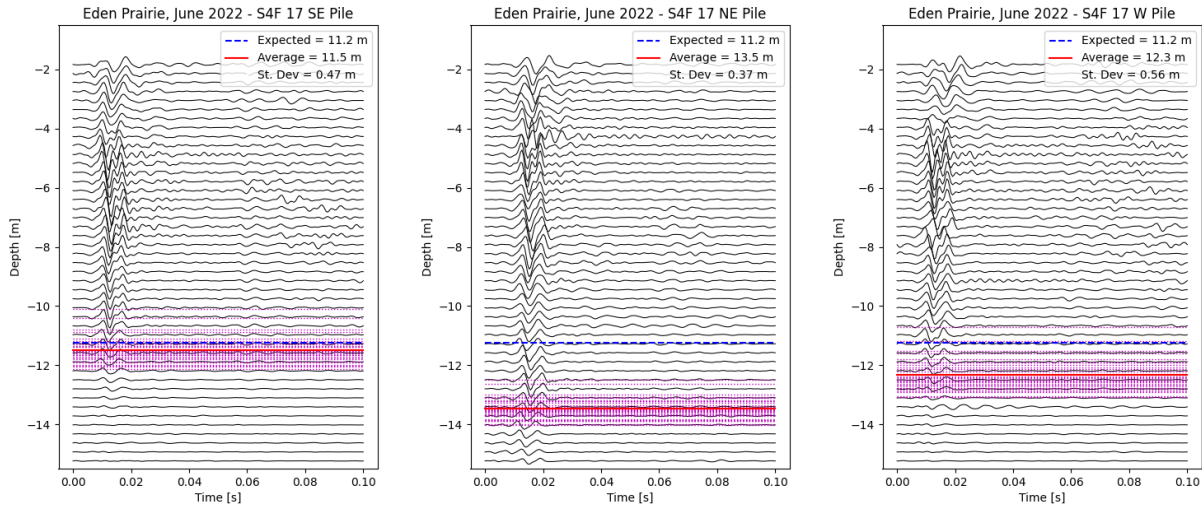
Figure 5.15 HMLT S4F-17 hammer impact results; left = SE Pile, middle = NE Pile, right = W Pile.

During the HMLT foundation testing on June 1, 2022, soil stratigraphy information for the HMLT S4F-17 site was collected with the CPT rig. One standard CPT test (c200) was performed at the tower site. Figure 5.16 shows the soil stratigraphy at the tower foundation. A mixture of SBT 4 – 9 (silt/sand mixtures, sands, gravely/stiff sand) is seen from the surface to a depth of 15 ft. Past a depth of 15 ft the predominant soil type is SBT 6, clean sand to silty sand, with sand mixtures (SBT 5) starting at a depth of 45 ft. The pore pressure results show that the groundwater level is at a depth of around 20 ft.
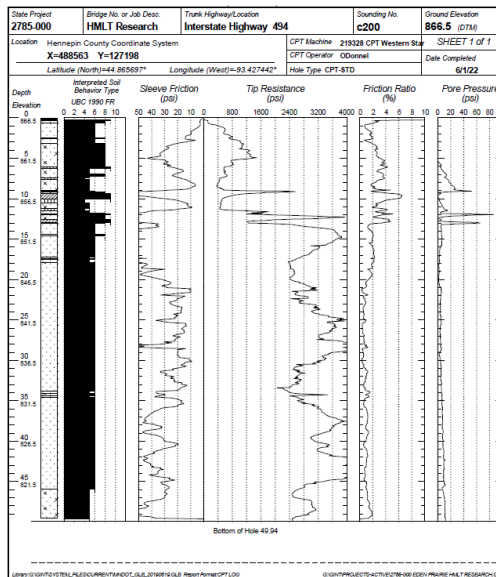

Figure 5.16 c200 CPT results at HMLT S4F-17.

HMLT Pole ID: S4F-15 was nondestructively tested on June 2, 2022. Tower S4F-15, a T-120 tower, is in the northwestern quadrant of the I-494 / TH 212 interchange in Eden Prairie, MN. Like HMLT S4F-17, only the hammer impact method of pile depth analysis was implemented at HMLT S4F-15. Figure 5.17 shows the location of HMLT S4F-15 and images from field testing.

Figure 5.17 HMLT S4F-15 location.

One pile, which points to the north, was evaluated with the hammer impact method of analysis. The 'High Mast Light Tower database MDH' excel file, provided by MnDOT, shows recorded pile length of 38.4 ft (11.7 m) for HMLT S4F-15. There was 2.5 ft of soil between the ground surface and top of the pile cap during testing. Again, including the 1.5 ft of concrete pile cap above the pile's uppermost insertion point and the 7.125° inclination of the pile, this gives an estimated pile embedment depth of 42.1 ft (12.8 m). The field-testing results for the pile is shown in Fig. 5.18. In the Figure, the estimated pile depth (based on tower database and pile cap geometry information) is highlighted with a blue dashed line; dotted maroon and solid red lines indicate the neural network outputs, similar to section 5.2.1.
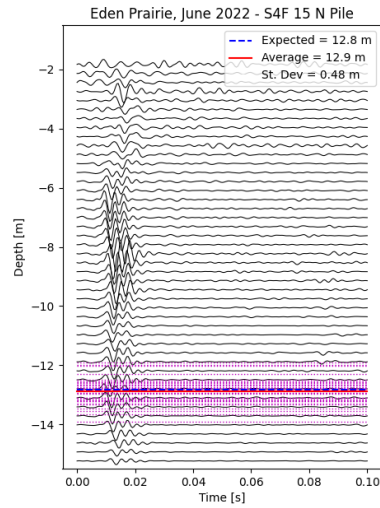
Figure 5.18 HMLT S4F-15 hammer impact result.

During the HMLT foundation testing on June 2, 2022, soil stratigraphy information for the HMLT S4F-15 site was collected with the SCPT rig. One standard CPT tests (c201c) was performed at the tower site. Figure 5.19 shows the soil stratigraphy at the tower foundation. From the surface to a depth of 10 ft the soil is mainly SBT 6, clean sand to silty sand. From 10 ft to 20 ft the soil is mostly SBT 5, silty sand to sandy silt. From a depth of 20 ft to the bottom of hole at 49.62 ft the soil is a mixture of SBT 5 and SBT 6. The pore pressure results show that the groundwater level is at a depth of around 15 ft.
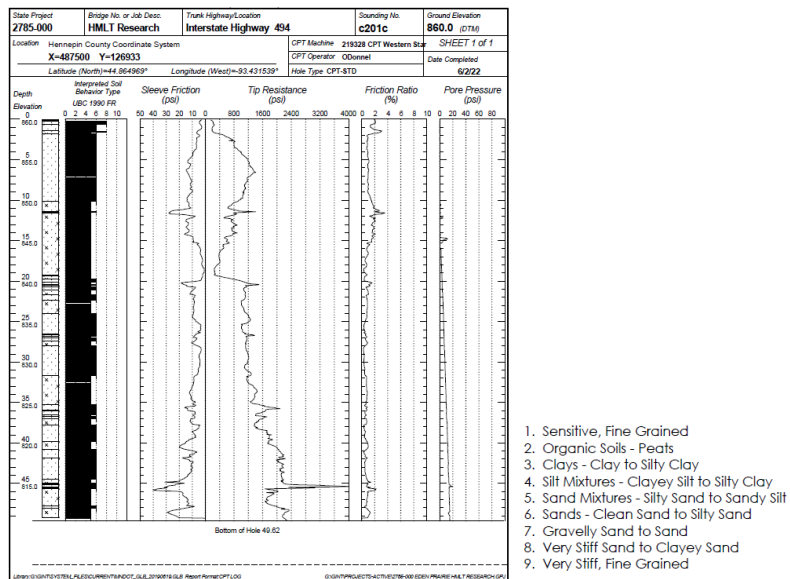

Figure 5.19 c201c CPT results at HMLT S4F-15.

CHAPTER 6: CONCLUSIONS

This report establishes non-destructive field-testing techniques, including data analysis algorithms, for determining in situ pile embedment depths by way of seismic waves. It is estimated that a possible benefit to Minnesota taxpayers of more than $8 million in foundation replacement costs could be realized with the development of non-destructive evaluation (NDE) techniques for determining the in situ pile lengths. The embedment depth of each pile supporting an HMLT is identified through a systematic sensing approach that includes (i) collection and classification of pertinent foundation designs and soil conditions; (ii) 3D simulations of dynamic soil-foundation interaction; (iii) parametric studies of the 3D pile sensing problem; (iv) field testing, and (v) analysis driven data interpretation using machine learning (ML) algorithms. The key in the development of the methods is the recognition that each pile serves, due to the high impedance contrast between the pile and soil, as a *waveguide*, facilitating the transmission of mechanical energy all the way to the bottom of the pile, and as a *mechanical antenna*, where the wave energy propagating down the pile is partially radiated into the surrounding soil. For robustness of the pile depth estimates, the envisioned field procedure entails the application of both transient (hammer impact) and steady-state (shaker) excitation of the pile cap, while monitoring the induced ground motion via a seismic cone penetrometer (SCP) along a vertical line close to the pile being interrogated. In this regard, this investigation highlights: (i) development of a finite element analysis (FEA) platform to simulate the visco-elastic waves generated in the pile cap, the piles, and the soil, and (ii) implementation of machine learning (ML) algorithms, trained using the outputs of FEA simulations, used to interpret the vertical ground motion profiles (as captured by the SCP) toward estimating the in situ pile depth. The featured ML algorithms are implemented as deep neural networks within the *Keras* and *TensorFlow* environment, to enable a robust yet computationally-efficient interpretation of the vibratory and hammer impact data.

Multiple HMLT pile foundations in the Twin Cities metro area were successfully tested from September 2020 through June 2022. During testing, both steady state and hammer impact testing methods were implemented to determine the in situ pile embedment depth of the tower foundations. To prepare the site for field testing, a preliminary investigation procedure was developed and implemented, providing the orientation and geometry of the in-ground pile cap, thus giving guidance on optimal locations for the testing hardware and CPT truck. The results obtained for HMLT E3A-11 in Mendota Heights, Minnesota, show a clear and significant change in the ground motion for both testing methods at depths between 10 m and 11 m. Comparing the results of the field testing to pile lengths provided by MnDOT's High Mast Light Tower database MDH excel file showed that the results obtained during testing at HMLT W1L-5 in Burnsville, Minnesota, closely matched the expected pile depth for the hammer impact method but were less conclusive for the vibratory source method. Results from testing at HMLT R19J-7 in Shakopee, Minnesota, showed that the hammer impact analysis for Pile 1 both (i) gave similar repeatable results (tested in November 2021 and retested in May 2022) and (ii) has outputs from the ML neural networks that were a close match to the expected pile depth. Again, the testing results and corresponding output from the ML network were less conclusive for the vibratory method on Pile 1 of HMLT R19J-7. For Pile 2 of HMLT R19J-7, both the hammer impact and vibratory source analysis methods gave ML network predicted depths that were consistent with each other, but roughly 2 to 2.5 m shorter than the expected pile embedment depth. Field testing of HMLT S4F-17 in Eden Prairie, Minnesota, specifically focused on

the hammer impact analysis. It was demonstrated that a traditional CPT test and the hammer impact evaluation of all three piles for HMLT S4F-17 could be conducted in a single day of field testing. Outputs from the hammer impact analysis of HMLT S4F-17 showed a good match between the predicted and expected pile depth for the SE pile, while the NE and W piles had predicted depths that were somewhat deeper than expected. A second tower, HMLT S4F-15, in Eden Prairie, Minnesota, was also evaluated using only the hammer impact method. The results from the field testing and corresponding output from the ML neural network showed a close match between predicted and expected pile depth. Overall, the results indicated that the hammer impact method provided closer and more consistent outputs for the predicted pile depth of the HMLT foundations than the vibratory method. In addition, by only implementing the hammer impact method, it was shown that an entire HMLT (3 piles) can be nondestructively evaluated, including performing a CPT soil analysis, in a single day of testing.

REFERENCES

[1] Modeling of linear dynamic damping – Code Aster. Retrieved from
https://www.code-aster.org/V2/doc/v14/en/man_r/r5/r5.05.04.pdf

[2] Operator DYNA VIBRA – Code Aster. Retrieved from
https://www.code-aster.org/V2/doc/v13/en/man_u/u4/u4.53.03.pdf

[3] Operator DEFI MATERIAU – Code Aster. Retrieved from
https://www.code-aster.org/V2/doc/v13/en/man_u/u4/u4.43.01.pdf

[4] Lindfield, G. R., & Penny, J. (2019). *Numerical methods: Using MATLAB*. Cambridge, MA: Elsevier,
Academic Press.

[5] Operator DYNA_LINE_TRAN – Code Aster. Retrieved from
https://www.code-aster.org/V2/doc/default/en/man_r/r5/r5.05.02.pdf

[6] Elements of absorbing border – Code Aster. Retrieved from
https://www.code-aster.org/doc/default/en/man_r/r4/r4.02.05.pdf

[7] Palachy, S. (2019, September 16). Understanding the scaling of L^2 regularization in the context of
neural networks. *Towards Data Science.* Retrieved from
https://towardsdatascience.com/understanding-the-scaling-of- l²-regularization-in-the-context-
of-neural-networks-e3d25f8b50db

[8] Rumelhart, D. E., Hinton, G. E., & Williams, R. J. (1986). Learning representations by back-propagating
errors. *Nature*, 323(6088), 533-536. https://doi:10.1038/323533a0

[9] Chollet, F. (2018). *Deep learning with python*, Second edition. Shelter Island, NY: Manning
Publications

[10] Keras documentation: About Keras. Retrieved from https://keras.io/about/

[11] Kingma, D. P. & Ba, J. (2014). Adam: A method for stochastic optimization.
Paper presented at the 3rd International Conference for Learning Representations, San Diego